

POLITECNICO DI TORINO

Corso di Laurea Magistrale in Ingegneria Civile

Tesi di Laurea Magistrale

Probabilistic river flood modelling and mapping

Case study: Dender



Relatore

Prof. Fulvio Boano

Correlatore

Prof. Carlo Camporeale

Supervisor (Katholieke Universiteit Leuven - Belgium)

Prof. Patrick Willems

Candidata

Gabriella Mangione
s222143

a.a. 2017-2018

Table of contents

List of figures	III
List of tables	V
Riassunto in italiano	VI
Introduction	1
1. Modelling tools	
1.1 Overview of flood forecasting modelling chain	6
1.2 Hydrological and hydrodynamic model	9
1.2.1 Description hydrological model (NAM)	9
1.2.2 Description river models: MIKE11 model and conceptual model	11
2. Case study of the river Dender	
2.1 Description case study	23
2.2 Results NAM model and comparison with observations	27
2.3 River model results	32
2.3.1 MIKE11 results	32
2.3.2 Conceptual model results vs MIKE11 results	36
3. Uncertainty in river modelling	
3.1 Uncertainty quantification	41
3.2 Propagating uncertainty through model	46
4. Probabilistic flood mapping	
4.1 Methodology	51
4.2 Source of uncertainty of the case study: incoming discharge from Wallonia	54
4.3 Results	56
Conclusions	66
	I

Appendix	67
Bibliography	69
Sitography	73

List of figures and tables

List of figures

Figure 1 – Plan and cross section views of river flood zones (Source: Adbpo)	3
Figure 2 – Hydrological and hydrodynamic model	9
Figure 3 – Structure of the NAM model	11
Figure 4 – Schematization of the conceptual model of the river Dender network (ch. from 4900 to 5769). The central reservoir represents the river Dender, while the upper and lower reservoirs are the floodbranches used to model the floodplains.	14
Figure 5 – Example of hypsometric curve (storage- water level relation)	15
Figure 6 – Backwater profile in a subcritical flow	17
Figure 7 – Scheme of conceptual modelling approach	18
Figure 8 – Map of the Dender basin and main cities in the basin. (Source: Grenzeloze Schelde)	24
Figure 9 – Subcatchments of the Dender basin	26
Figure 10 – NAM results	27
Figure 11 – Locations of the available measurement nodes	28
Figure 12 – Comparison: Opwijk, Vondelbeek	28
Figure 13 – Comparison: Essene, Bellebeek	29
Figure 14 – Comparison: Aalst, Molenbeek	29
Figure 15 – Comparison: Iddergem, Molenbeek	30
Figure 16 – Example of graph containing simulated and observed discharges in case of perfect agreement (blue line) and reality (red line)	31
Figure 17 – Simulated and observed discharges for catchment 430 (Aalst, Molenbeek)	31
Figure 18 – Comparison: Left bank / water level (MIKE results)	34

Figure 19 – Comparison: Right bank / water level (MIKE results)	34
Figure 20 – Flood map near Geraardsbergen	35
Figure 21 – Time series of the discharge in Overboelare (Geraardsbergen) from January 2010 to February 2018	36
Figure 22 – Water level results of MIKE11 model and conceptual model (Left: November 2010, Right: January 2011), chainage: 3365	38
Figure 23 – Water level results of MIKE11 model and conceptual model (Left: November 2010, Right: January 2011), chainage: 39815, transition zone	38
Figure 24 – Water level results of MIKE11 model and conceptual model (Left: November 2010, Right: January 2011), chainage: 45810, tidal zone	38
Figure 25 – α -cut of a fuzzy set	43
Figure 26 – Errors versus simulated water levels (catchment Viaene)	46
Figure 27 – a) Confidence intervals of upstream boundary, b) Water level results in the Dender and c) Water level results in a floodbranch	49
Figure 28 – a) Deterministic and b) probabilistic flood map	53
Figure 29 – Nearest-neighbour interpolation used in flood raster	57
Figure 30 – Identification and comparison between water level and DEM values at a given location	58
Figure 31 – Locations of the produced PFMs	59
Figure 32 – PFM of the area at the south of Geraardsbergen (flood event of January 2011)	60
Figure 33 - PFM of the area between Geraardsbergen and Ninove (flood event of January 2011)	60
Figure 34 – Inundation areas of the last twenty years (from helicopter images) near Overboelare	61

Figure 35 – Inundation areas of the last twenty years (from helicopter images) between Geraardsbergen and Ninove	62
Figure 36 – Deterministic flood map (MIKE11 simulation) superimposed on the topographic map near Overboelare (flood event of June 2016)	63
Figure 37 – GIS visualization of PFM, area at the south of Geraardsbergen (flood event of January 2011)	64
Figure 38 – GIS visualization of PFM, area between Geraardsbergen and Ninove (flood event of January 2011)	64

List of tables

Table 1 – ID and areas of the catchments of the Dender basin	25
Table 2 – Two-dimensional error matrix	45
Table 3 – Matlab commands for construction of confidence intervals	48
Table 4 – Storage reservoirs that compose the conceptual model of the river Dender	68
Table 5 – Methods used to calculate water levels and discharges	68

Riassunto in italiano

Negli ultimi decenni, sia il mondo scientifico che le diverse autorità che si occupano di protezione del territorio e in particolare di eventi di piena hanno elaborato vari modelli in grado di prevenire inondazioni e limitare i danni che ne conseguono. La presente tesi analizza diversi possibili tipi di modellazione idraulica dei fenomeni di inondazione, con riferimento al caso studio del fiume Dender, situato in Belgio.

Nella prima parte, il modello idrodinamico implementato nel software Mike11 è utilizzato per risolvere le equazioni complete di de Saint-Venant. Questo tipo di modellazione fornisce risultati accurati ma richiede tempi lunghi di simulazione, tempi che invece risultano quanto mai ristretti in caso di eventi estremi. Per ovviare a tale problema e cercare di ridurre i tempi di calcolo, viene preso in considerazione un metodo alternativo di modellazione, dato dai modelli concettuali.

I risultati ottenuti dalle precedenti simulazioni vengono quindi confrontati al fine di valutare se l'utilizzo dei modelli concettuali porti a una perdita di accuratezza significativa o meno. Viene riscontrata una quasi esatta corrispondenza fra i risultati, le cui differenze risultano avere ordine di grandezza non maggiore delle incertezze stesse. La considerazione che ne deriva è che il modello concettuale utilizzato nella presente tesi rappresenta una alternativa più rapida ma allo stesso tempo ugualmente efficace rispetto ai modelli idrodinamici dettagliati.

Dati i tempi di calcolo estremamente ridotti, si utilizzano pertanto i modelli concettuali nella seconda parte di tesi, dove c'è la necessità di eseguire simulazioni multiple. In quest'ultima parte, infatti, si prendono in considerazione i diversi tipi di incertezza: incertezza sui dati di input, incertezza sui parametri e incertezza intrinseca dovuta a imperfezioni di modello. Si modificano le condizioni al contorno e si procede alla propagazione delle incertezze, la quale porta a differenze significative in termini di risultati finali.

Dal momento che nessun modello è mai del tutto esente da incertezza, si può dedurre che i sistemi di gestione e previsione delle inondazioni possono

generare mappe di inondazione deterministiche potenzialmente sbagliate. Tale problema può essere in parte risolto tramite la produzione di mappe di inondazione probabilistiche, ovvero mappe costituite da linee indicanti uguale probabilità di allagamento. Queste mappe offrono dunque un'ulteriore informazione, che diviene possibile grazie alla propagazione delle incertezze effettuata nel precedente step.

Introduction

The issue of flood risk has to be managed properly, since flooding can lead to several damages: loss of life, physical injury but also economic losses, electricity supply cut off, damage to assets and infrastructures (including disruption of services). It can also have significant impacts on the environment, such as erosion or degradation of water quality. Alderman *et al.* (2012) analyze the relationship between floods and human health. They list both short- and long-term health outcomes due to flood events, that consist not only of mortality due to drowning but also of: toxic exposure due to chemicals in the environment that can be released, contamination of drinking water facilities, damage to water supply systems, as well as increased risk for water-borne and vector-borne diseases.

There are different types of flood: river floods, estuarine-coastal floods and urban floods (Van Steenbergen, 2014). The specific case of river flood occurs when the capacity of the embankments is exceeded, as a result of an intense and prolonged rainfall. Estuarine-coastal floods are primarily due to sea-level rise and are exacerbated by changes in storm frequency and intensity, as a result of climate change (Ramsay *et al.*, 2017). Growing coastal hazards depend on mean sea level in combination with high tide, storm surge (i.e. temporary rising water caused by winds and low pressure), tsunami, wave overtopping (that occurs when waves exceed the barrier elevation, which can be a berm, a seawall or the natural crest of the beach). Lastly, urban floods are the consequence of a lack of drainage in cities. Paved surfaces mean low infiltration, therefore the whole rainfall is transformed into runoff. If the sewage system or the draining canals do not have sufficient capacity, this may lead to water level rising in the city streets.

The main causes of floods are long rainfall periods and/or high intensity rainfall, but consequences can get worse depending on antecedent conditions of the ground, land use, thoughtless urbanization and city planning, low drainage capacity, geology, vegetation and soil type, steep slopes that cause fast surface runoff. Furthermore, flood risk is expected to increase due to climate change and socio-economic development. The influence of climate change on river flood risk has been assessed by Arnell and Gosling (2016), who consider four

indicators of the flood hazard. The first one is the flood frequency, which is going to change due to change in both the return period and the magnitude of flood peaks. The second one is the population exposed to change in flood hazard, which is calculated by considering people living in flood-prone areas. The third one is the cropland exposed to change in hazard. The last indicator is the flood risk, that takes into account the relation between the flood magnitude and the flood loss. The impacts can be estimated using a hydrological model with a chosen grid resolution and considering different climate models that lead to different scenarios. However, changes in flood characteristics depend not only on the global mean surface temperature, but also on the type of environment. For instance if floods in a certain region are mainly caused by intense rainfall but the infiltration capacity of the soil is not important, the change in precipitation has a great impact on these territories. On the contrary, if the saturation factor is relevant, floods are influenced by both rainfall and evaporation.

The correct approach to flood management considers both structural and non-structural measures. The former include embankments or hydraulic structures like gates, sluices, retention basins, detention basins, infiltration basins, dams. The latter include flood plain zoning, flood forecasting and warning systems. Flood plain zoning is notably a measure that tries to reduce flood consequences by placing restrictions on land use. In this way building and development in flood plains are limited. Different zones are identified and classified according to the severity of risk, and only certain types of activity/facility (e.g. hospitals, parks, playing fields, schools, offices, industrial or residential areas) are permitted in each zone. Many countries around the world rated the areas surrounding rivers and each of them has its own classification. For example in Italy the PAI (“Piano per l’Assetto Idrogeologico”, i.e. Hydrological Structure Plan) defines flood risk maps and it also includes the necessary measures to reduce the impacts that extreme weather events can have on geomorphologically hazardous areas. It is a tool for soil use management and urban planning. The PAI classifies the area surrounding a river in three zones:

- A zone, Flood outflow zone (Fascia A, fascia di deflusso della piena): the area where the 80% of the peak discharge flows, given a return period of 200 years.

- B zone, Flooding zone (Fascia B, fascia di esondazione): the area where the DEM values are greater than the water levels corresponding to a peak discharge with return period of 200 years. It is the area within the embankments.
- C zone, Catastrophic zone (Fascia C, fascia di inondazione per piena catastrofica): the area where a peak discharge corresponding to a return period of 500 years flows.

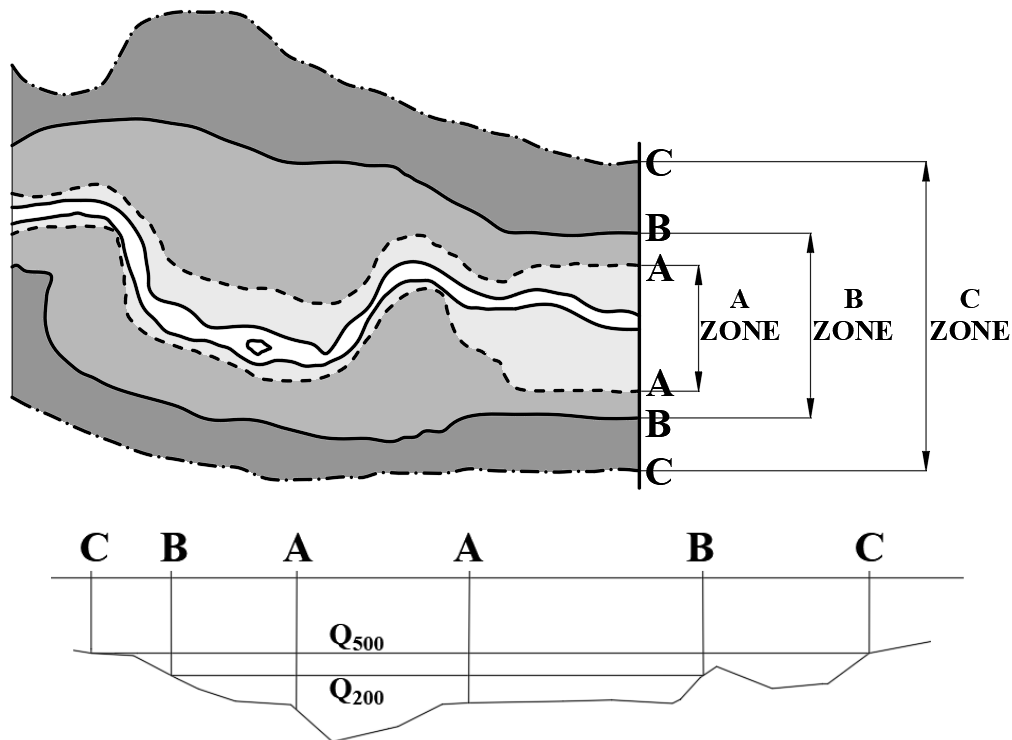


Figure 1 – Plan and cross section views of river flood zones (Source: Adbpo)

Since this thesis will focus on a case study located in Flanders (Belgium), here there is an overview of the different types of flood plain maps that are developed in this region (Source: European Commission).

- NOG-maps (Naturally flooded area maps): they indicate the areas that are likely to be flooded, considering the soil-maps (that show both river sediments and gravity-caused sediments).
- ROG-maps (Recently flooded area maps): they result from the cooperation of water authorities, provinces and municipalities, who produced recently flooded areas by making use of cartography, photographs, DTM data.
- MOG-maps (Modelled flooded area maps): they are the most detailed maps and are generated using hydrological and hydrodynamic models. Flood

extents and flood depths associated with specific return periods are computed.

Other examples of flood maps produced in most EU Member States can be found on the website of the European Commission. Indeed in 2006 the European Water Directors decided to create a circle of experts from 24 European countries to promote the exchange of information about flood mapping. This led to the production of a Handbook of good practices in flood mapping, including an Atlas of Flood Maps. The European Commission website also includes the links to the main internet sites developed by each country, which are occasionally updated. Aware of the likely higher flood risk in Europe in the future, the European Commission defined the steps for an effective flood risk management (which are the basis of the Directive 2007/60/EC):

- Prevention: placing restrictions on building in flood-prone areas and facilitating infiltration in order to reduce the surface runoff. However, some measures are not possible in case of already developed floodplains.
- Protection: taking structural and/or non-structural measures.
- Preparedness: enhancing public information and awareness about flood risk and giving recommended rules of behavior in this case.
- Emergency response: preparing response plans containing the most appropriate steps to take if flooding occurs.

The last two steps are closely related to the calculation time required in the flood mapping phase. Indeed, calculation time plays a key role in flood forecasting, since the time available in these situations is very limited. This is the reason why it would be impossible to use detailed hydrodynamic models (like MIKE11 or InfoWorks-RS) for real-time flood forecasting. More precisely, these models can make predictions but they cannot get the changes in the system and update the predictions considering the real-time observations. Indeed, the use of real time observations is crucial when one wants to produce more accurate predictions because real measurements gives an extra validation of the produced results. These measurements contribute to improve model results by adapting the model to changes as fast as they occur. The solution to this problem is to use the conceptual models, i.e. an alternative modelling technique which can significantly reduce the computation time. These models try to emulate the detailed models by using simplified equations. One of the aims of this thesis is to estimate the loss of accuracy resulting from the use of the conceptual models.

For this purpose, both the detailed model and the conceptual model simulations are performed and then compared. This means that for each type of model the entire flood forecasting modelling chain is carried out: the data acquisition, the hydrological model, the hydrodynamic model and finally the GIS visualization.

In order to understand all the necessary steps for this analysis, here there is an overview of the contents of this thesis. The first part of the thesis describes some of the possible modelling tools that can be used in flood modelling and that will be applied later to run simulations of one specific case study and for specific flood events. Firstly, the hydrological model considered in the simulations, the NAM model, is described. NAM is developed by the DHI (Danish Hydraulic Institute) and stands for Nedbør-Afstrømnings- Model, i.e. “precipitation- runoff-model”. Without going into details, it is a lumped, conceptual rainfall-runoff model that simulates the behaviour of the land phase by considering the moisture content in four interrelated storages: surface storage, lower zone or root zone storage, groundwater storage and snow storage (DHI, 2011). The meteorological data requirements are the rainfall and evapotranspiration. It calculates the runoff from the river basin to the waterways.

Secondly, the hydrodynamic model built in MIKE11 and the alternative technique of the conceptual river models are illustrated. The hydrodynamic model computes water levels and discharges in rivers and floodplains. Then the case study of the river Dender located in Flanders (Belgium) is presented. For this case study and for given flood events, the results of the hydrological model (NAM) and the ones of the hydrodynamic models (both MIKE11 model and conceptual river model) are discussed. After that, the different sources of uncertainty are listed and the problem of uncertainty quantification and its propagation is investigated. Finally, probabilistic flood maps, i.e. maps composed by lines with equal probability to be flooded, are produced, so that the aforementioned uncertainty can be accounted for.

Modelling tools

1.1 Overview of flood forecasting modelling chain

Flood forecasting and warning systems have been developed worldwide in order to minimize the consequences of flooding and to warn people and communities. These systems try to predict water levels and discharges in rivers and floodplains through the following steps:

1. **Rainfall and evapotranspiration data** – These values can either be observed or forecasted data. In Flanders the observed historical data and some predictions are available on the website *www.waterinfo.be*, which is the portal of the water managers where anyone can freely check current information as well as short-term and/or long-term forecasts about flooding and rainfall. On the contrary, the data that refer to the Walloon Region can be found on the website *http://voies-hydrauliques.wallonie.be*.

Rainfall measurements can be recorded by a pluviometer, which provides point rainfall data. In Flanders there are several tens of pluviometers that transmit the data to the *waterinfo* portal every 30 minutes. Otherwise estimates can be achieved by the analysis of real time radar images from the Royal Meteorological Institute. The RMI can thus calculate catchment area rainfall for the upcoming hours. Weather radars emit electromagnetic waves that propagate through the atmosphere and interfere with raindrops, snowflakes and other types of hydrometers (Biggs, 2011). Then they measure the back-scattered energy to estimate the potential precipitation intensity. This “Doppler weather radar” is an active remote sensing technique that finds a relationship between radar reflectivity and rainfall rate (Li *et al.*, 2016). However, one single ground-based station is not fit for a large number of applications. For this reason, over the last few years radar networks of a larger scale began spreading all over the world. The advantage of the estimates that come from weather radars is that they take into account the spatial variability of rainfall. On the other side, since they are indirect measurements, bigger uncertainty affects

them. For this reason rainfall input can be less accurate than the real measurements coming from gauge stations.

Another kind of hydrologic remote sensing technique consists of satellite retrievals. Indeed satellites provide observed precipitation data by means of continuous monitoring from space (Li *et al.*, 2016). Satellites exploit different types of sensors: the infrared technology is the basis of the thermal infrared sensors (TIR), which are usually installed on geostationary satellites; otherwise active or passive microwave sensing techniques can be used. The former estimate precipitation by measuring cloud-top temperature and then deriving the rainfall rate. On the contrary, microwave radiation can give more accurate results, as it can penetrate through clouds.

2. **Hydrological model** – This phase calculates the amount of water that flows to the river (output) starting from the amount of water that comes from the rainfall (input), including potential evapotranspiration (input). It simulates the hydrological processes and returns the runoff discharge. This step is highly influenced by the previous one. Indeed, the spatial distribution of rainfall strongly affects the hydrological model. The sensitivity of hydrological models to spatial rainfall variability has been studied by Arnaud *et al.* (2002), who applied different patterns of rainfall and assessed their influence on the estimation of flood probability. The study showed that both peak flows and runoff volumes may significantly differ according to the chosen pattern. Gabriele *et al.* (2017) propose a double information approach, which takes into account both rain gauges measurements and weather radar measurements. Merging these two types of information leads to more reliable rainfall estimations, especially in case of small catchments.
3. **Hydrodynamic model** – This model uses the runoff generated by the hydrological model as an input and, by means of the de Saint-Venant equations, computes water levels and discharges in rivers and floodplains. Different types of flood modelling are possible: one-dimensional, two-dimensional or three-dimensional. 1D hydraulic modelling assumes the existence of a single preferred direction of the flow and it also assumes that the flow slowly varies in the cross section of the river (Gharbi *et al.*, 2016). The full de Saint Venant equations are solved by programs like MIKE11 or HEC RAS using a finite difference method. Flanders

Hydraulic Research mainly uses 1D hydrodynamic models. This type of models is fast and good enough for floodplain flow and flood mapping; on the other side some of the major disadvantages are the need to identify major flow routes to set up the model and the limited capacity to simulate urban floods (CH2M, 2017). On the contrary, 2D hydraulic models make vertical integration since they assume an almost zero vertical velocity. Programs such as TELEMAC solve the 2D de Saint Venant model using a finite element method. 2D models usually require digital terrain model (DTM) or bathymetry of channels (CH2M, 2017). They are more accurate than 1D models, however they are slower and a fine grid needs to be specified for river channels. Sometimes, 1D and 2D modelling techniques are combined, where the former are used for channels, while the latter are used for floodplains. 1D and 2D domains are then linked.

MIKE11 (1D) can be used for river modelling, however it cannot include coastal areas: to model these areas a 2D or 3D model is necessary. Indeed, DHI developed MIKE21, which is the specific software for marine and offshore structures, coastal protection infrastructures, port layout optimization, coastal flooding, storm surge warning systems, water forecast for safe navigation (DHI, 2017). If necessary, it can include advanced modules for waves.

Finally, 3D models are never used for riverine areas, but only to model free surface flows of coast and sea. It is mostly used for ecological and environmental purposes.

4. **GIS visualisation** – It is a common practice to generate flood maps in order to predict the flood extent. These maps help water managers to minimize the damage during flood events but they are also useful for spatial planning and development of the urban settlement. Their use is becoming more and more important since the world population growth is leading to an increase in urban extent and therefore to a bigger exposure of the population, which is even more located in flood-prone areas. About that, the study by Muis *et al.* (2015) considers both climate change and urban expansion in the analysis of the increasing flood risk. Since GIS visualisation is a very useful tool to show potential inundation of flood-prone areas, Demir and Kisi (2015) give an overview of the main steps considered in this procedure. First of all, topographical data need to be digitized and ArcGIS is used to generate the digital elevation model

(DEM). A hydraulic model like HEC-RAS is then used to simulate the flood flows. The last step is to combine ArcGIS and HEC-RAS in order to obtain flood risk maps for given return periods.

1.2 Hydrological and hydrodynamic model

In this section both the hydrological and hydrodynamic models are described. In the first part of this thesis, the MIKE11 software, developed by the DHI (Danish Hydraulic Institute) Water & Environment, is used to solve both the hydrological model (NAM) and the hydrodynamic model. Then, the detailed hydrodynamic model will be replaced by a completely different modelling approach, the conceptual river model. Figure 2 contains an overview of the factors considered by the two models and that will be described later.

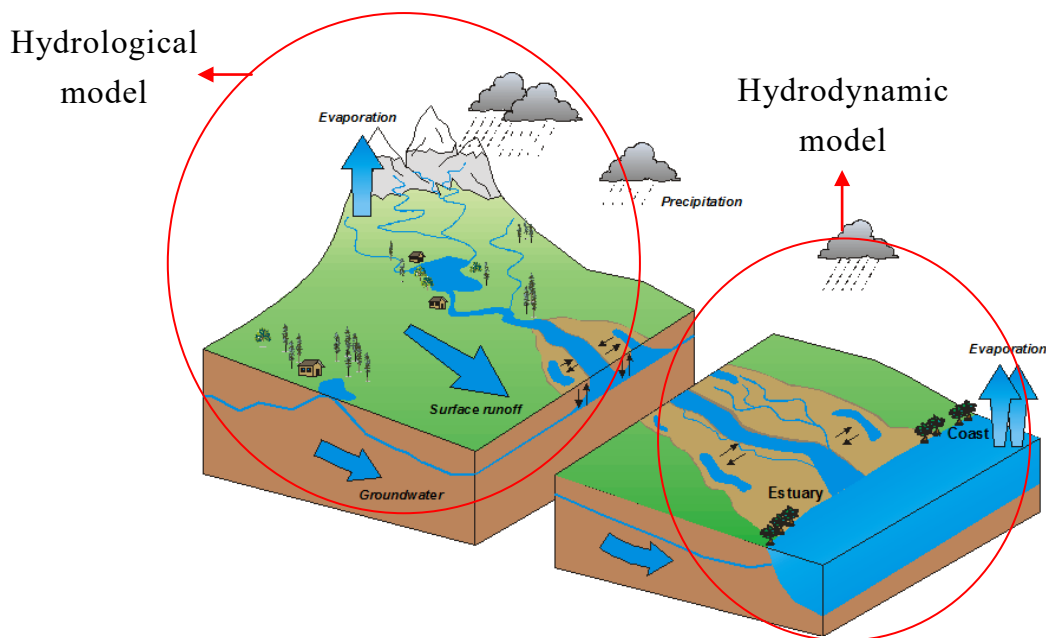


Figure 2 – Hydrological and hydrodynamic model

1.2.1 Description hydrological model (NAM)

Different types of Rainfall-Runoff models are available in MIKE11 (DHI, 2011). These models are:

- UHM (The Unit Hydrograph Module). It simulates the runoff from single storm events using unit hydrograph techniques in case there are no streamflow records.

- SMAP. It is based on the moisture storage in the root zone and in the groundwater and the interaction between these two storages.
- Urban. There are two different methods: the time/area method and the non-linear reservoir method. The former is founded on the initial loss, the continuous hydrological loss and the size of the area. The latter uses the kinematic wave computation.
- FEH (Flood Estimation Handbook). It is a standard used in the UK to estimate local flood risk.
- DRiFt (Discharge River Forecast). It is based on a geomorphologic approach and describes the different parts of the drainage system.
- NAM (Nedbør-Afstrømnings-Model, i.e. “precipitation-runoff-model”).

In this thesis the NAM model is considered. NAM is a lumped, conceptual rainfall-runoff model that describes the behaviour of the land phase, where each catchment is treated as a single unit. The NAM model calculates the overland flow, interflow and baseflow, depending on the moisture content of four mutually interrelated storages: surface storage, lower zone or root zone storage, groundwater storage and snow storage. For the simulations of this thesis the contribution of the snow storage is neglected. Since NAM is a lumped model, a set of parameters is associated with each catchment. These parameters are determined using physical data, but hydrological observations (like discharge values) are also used to calibrate and validate the parameters. In the NAM module it is also possible to take into account man interventions such as irrigation or groundwater pumping that cause significant variations in the hydrological cycle. This can be done by specifying additional time series of extra rainfall or groundwater abstraction representing pumping rates.

There are several modelling components describing the different storages which are defined by the DHI. The first parameter is the maximum water content in the surface storage, U_{MAX} . This is an index of the moisture present in the upper part of the ground, in depressions and of the water captured by the vegetation. When this value is exceeded the water flows as overland flow or infiltrates to the lower zone. The second parameter is L_{MAX} , i.e. the maximum water content in the root zone storage, whose moisture content is influenced by the transpiration of the vegetation. It recharges the groundwater storage and influences the overland flow and interflow. The overland flow, interflow and baseflow routing is determined by the time constants CK_{12} , CK_{IF} , CK_{BF} , since

the storages are supposed to react as linear reservoirs. The exceedance of threshold parameters TOF, TIF, TG determines the generation of the flows and the groundwater recharge. Another runoff parameter that needs to be specified is CQOF, which indicates the extent to which excess rainfall becomes overland flow.

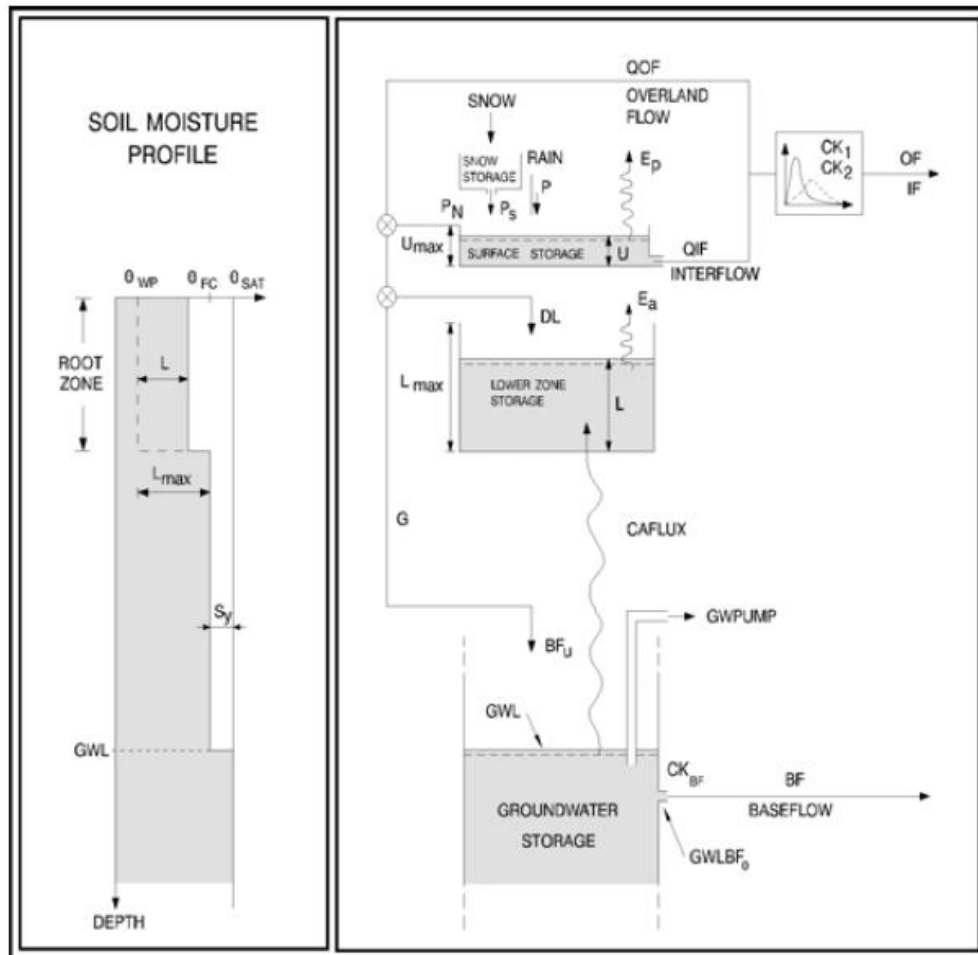


Figure 3 – Structure of the NAM model

1.2.2 Description river models: MIKE11 model and conceptual model

The following paragraphs describe the main features that characterize the two river models used in this thesis. The first part contains a brief explanation of the equations on which the hydrodynamic model is based, while the second part focuses on the delineation of the conceptual river models.

- **MIKE11 model**

The hydrodynamic model built in MIKE11 computes unsteady flows in river and estuaries. It solves the de Saint-Venant equations, assuming that the water is incompressible, the bottom slope is small and the pressure variation is hydrostatic (DHI, 2011). Including the hydraulic resistance and the lateral inflow, the integration of the mass and momentum conservation equations yields:

$$\frac{\partial Q}{\partial x} + \frac{\partial A}{\partial t} = q \quad (\text{Eq. 1})$$

$$\frac{\partial Q}{\partial t} + \frac{\partial \left(\alpha \frac{Q^2}{A} \right)}{\partial x} + gA \frac{\partial h}{\partial x} + \frac{gQ|Q|}{C^2 AR} = 0 \quad (\text{Eq. 2})$$

Where Q is the discharge, A is the flow area, q is the lateral inflow, h is the stage above datum, C is the Chezy resistance coefficient, R is the hydraulic radius, α is the momentum distribution coefficient.

According to the Abbott-scheme, the (Eq.1) and (Eq.2) are transformed into implicit finite difference equations by means of a computational grid where alternating points of discharges (Q) and water levels (h) are located.

For each simulation, it is possible to choose between three types of wave approximation (DHI, 2011):

- the dynamic (fully or high order fully dynamic) wave, which considers the full momentum equation and is capable of taking into account backwater effects, fast transients, tidal flows and all those cases where acceleration forces become significant
- the diffusive wave, which neglects the acceleration forces and only considers the terms due to gravity force, bed friction and hydrostatic gradient
- the kinematic wave, which is based on the balance between gravity and friction forces.

In this thesis the fully dynamic wave approach is used. This is because the diffusive and kinematic waves are simplifications of the dynamic one, therefore their use should be only limited to those cases when the magnitude of the neglected terms is not significant. However for the case study considered in this thesis (i.e. the river Dender) this cannot be assumed, since there are significant backwater effects that are caused by the hydraulic structures present all along the river.

The hydrodynamic model can only simulate a 1D flow but fictitious floodbranches can be implemented all along the river, so that it is possible to investigate the flow conditions in floodplain.

- **Conceptual river model**

The detailed hydrodynamic models, such as the MIKE11 HD model that will be used in the first simulation of this thesis, can provide an accurate solution of water levels and discharges by solving the full de Saint-Venant equations. However, this type of models are time consuming and the MIKE11 model requires on average half an hour to simulate one month of data (although with some variations depending on the specific technical features of the computer that is used). The calculation time is definitely an issue in real-time flood forecasting, indeed the reduction of calculation time can let flood forecasters run multiple simulations so that the control of hydraulic structures and the set-up of retention basins can be improved.

For this purpose a new modelling technique is proposed as an alternative to the detailed “white-box models” (Willems, 2000): the conceptual models. These “grey-box models” try to simulate the detailed models but use simplified relations in order to reduce the calculation time up to 2000 times if compared with MIKE11 simulations. Their level of detail is lower than the physically-based models, where mathematical equations describe the real world processes in the most accurate way. The basic idea of conceptual modelling is to schematize the river network by concatenation of reservoir elements. In this thesis the conceptual model developed by Meert *et al.* (2016) is used. It contains the delineation of the storage reservoirs that schematize the river Dender network. The Dender case study will be described in detail in the next chapters, however the following figure is very useful to understand the structure of the conceptual model. The river reach shown below is the one between chainage

4900 and 5769, which means a length of approximately 1 km. The central reservoir is the schematization of the river Dender, while the two other reservoirs (FBR 9 and FBR 10) represent the floodbranches: the latter are used to model the floodplains. Finally, there is a series of link channels which represent the embankments: in case of flood the outflow discharge flows through the link channels towards the floodplains.

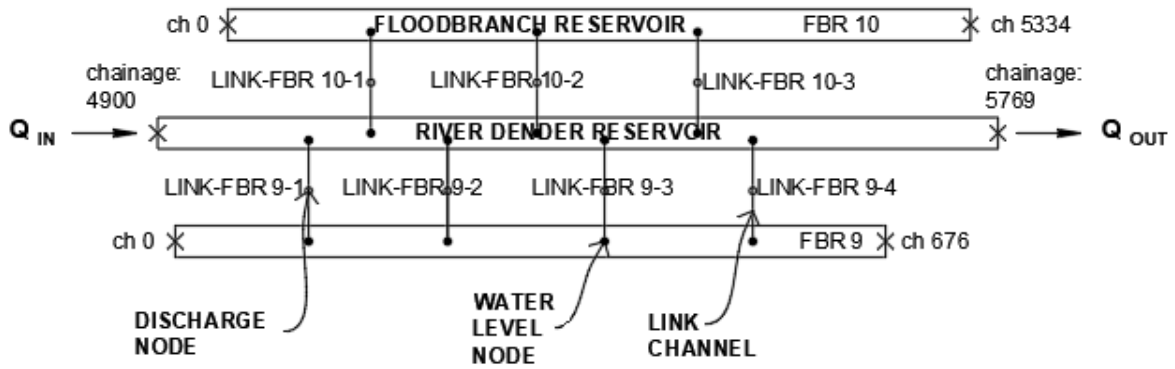


Figure 4 – Schematization of the conceptual model of the river Dender network (ch. from 4900 to 5769). The central reservoir represents the river Dender, while the upper and lower reservoirs are the floodbranches used to model the floodplains.

The differential equation used in the conceptual modelling approach is the one used by Fenton (1992):

$$\frac{\partial S}{\partial t} = I(t) - Q(t, S) \quad (\text{Eq. 3})$$

Where S is the water volume in the reservoir, t is the time, I is the inflow discharge and Q is the outflow discharge.

Eq. 3 is then approximated by:

$$S(t) = S(t-1) + \Delta t \cdot [I(t-1) - Q(t-1)] \quad (\text{Eq. 4})$$

where Δt is the calculation time step.

After the mass balance by means of Eq. 4, where all the different sources of the incoming flow (discharge from upstream reaches, from boundary data and from rainfall runoff links) and all the possible outflows are calculated, the storage at the current time step can be obtained.

Meert *et al.* (2016) give an overview of all the calculation modules that are required when a conceptual modelling approach is considered. Once the mass balance is closed and the storages in all the reservoirs are known, the water level

values need to be determined. This is done by using different relations according to the type of the reach in hand. The basic relation between the storage and the water level is the hypsometric curve, that can be used when backwater effects are negligible and for the reservoirs that represent the floodplains. Indeed, in case a static water level can be assumed, there is a unique relation between the water level and the storage volume. This relation is calibrated by means of the full hydrodynamic model simulations and is based on the Digital Elevation Model included in the MIKE11 files. The calibration is done by referring to one or more historical events with a certain return period. Extreme storms need be considered so that floodplains are flooded and thus the whole model can be calibrated. The following figure shows how the hypsometric curve looks like, if there are no backwater effects: in general it shows an approximately linear behaviour.

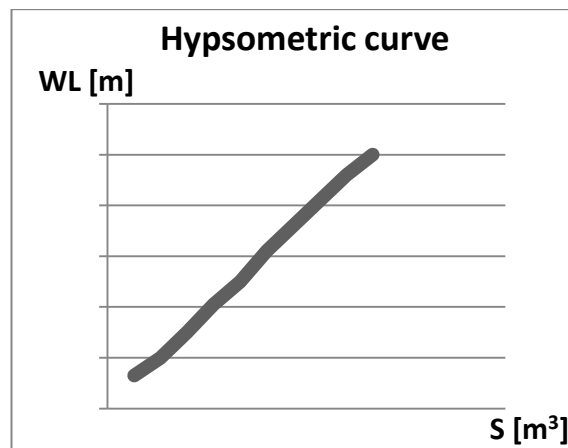


Figure 5 – Example of hypsometric curve (storage- water level relation)

A 1D-interpolation, that considers a piecewise linear function, is used to approximate this relation. Such a linear interpolation is recommended unless the backwater effects become significant. Otherwise, it is necessary to consider the influence of the downstream gate level. The Encyclopaedia Britannica defines a gate as a movable barrier for controlling the passage of fluid through a channel. It is a controllable hydraulic structure that can increase or decrease the volume of the flow. When the structure is closed, an obtuse angle pointing upstream is formed by the gates, so that higher resistance to the water pressure can be achieved. The main difference between a gate and a weir is that the gate is an adjustable structure that can be regulated, while the weir is a fixed structure over which water may flow. They are both used to control the upstream water level. In case of backwater effects caused by a downstream gate, the

hypsothetic curve is no longer suitable, whereas the use of the hypsothetic surface allows to take into account both the storage and the gate level states. This means that the graph in Figure 5 is replaced by a 3D graph with the following three axes: storage, water level and gate level. In MATLAB a 2D-interpolation is done by an algorithm that is capable of modelling a surface starting from scattered data.

Moreover, the hypsothetic curve cannot be applied to the tidal zones, where the downstream water level influences the whole reach. In these zones the hypsothetic curve will show a hysteresis, due to the fact that the water level variations and storage variations don't occur at the same time, as assessed by Meert *et al.* (2016). This problem can be overcome by relating the water levels at the current time step with the storage at the previous time step.

The transition zones need a separate analysis as well, since here the water surface profile is influenced by both the incoming discharge and the tidal wave. The direction of the flow regime is not the same in case of possible tides: during the flood, the flow regime goes upstream, whereas during the ebb it goes downstream. However, the tidal wave decreases its velocity during the propagation because of the frictional damping. Yankovsky *et al.* (2012) also hypothesize that enhanced bathymetric gradients characterise the transition zone, that is a further contribution to the dissipation. On the contrary, the freshwater inflow increases its velocity because of the smaller cross-sectional area. Yankovsky *et al.* (2012) define the transition zone as the segment of the river channel with comparable tidal and fluvial velocities.

The distinction between the static and the dynamic component of the storage is a possible solution to this problem. In case of tidal influence, the dynamic component is higher for the downstream part of the reach.

A black box model can be ultimately used for all those reaches which show a peculiar behaviour due to the presence of numerous hydraulic structures or in general due to changing flow conditions. For instance, in the specific case of a reservoir influenced by multiple factors, Meert *et al.* (2016) propose a second order polynomial where the water level is a function of the storage, gate level and discharge.

In the conceptual modelling approach, once the water level is known, the discharge can be calculated. The easiest method consists of using the storage-

outflow relation and can be applied in case the flow is not influenced by backwater effects. Otherwise, two alternative methods are possible. The former makes use of hydraulic structures and can use the same equations that are implemented in MIKE11. The latter consists of fictitious structures that are introduced when the backwater effects are significant even if any real hydraulic structure is present. In this case the equation that describes the energy head loss between two water level nodes is:

$$\left(h_1 + \frac{Q_1^2}{2gA_1^2} \right) - \left(h_2 + \frac{Q_2^2}{2gA_2^2} \right) = \Delta F \quad (\text{Eq. 5})$$

Where h is the water level, Q is the discharge, A is the cross-sectional area and ΔF is the energy head loss. ΔF is a function of the discharge Q , the hydraulic radius R , the area A , the length L between two water level nodes h_1 and h_2 and the bottom friction, which can be expressed by means of the Manning's coefficient n or Chezy constant, C . Indeed, in case of backwater effects, the discharges at two nodes, Q_1 and Q_2 , are different. The National Oceanic and Atmospheric Administration defines the backwater effect as the effect which a dam or other obstruction or construction (weir, bridge etc.) has in raising the surface of the water upstream from it. However, water can be backed up not only because of an obstruction, but also because of an opposing current or the tide. Hence it is possible to treat the backwater effect as if a fictitious structure is present. The following figure shows the typical backwater profile in a subcritical flow (mild slope). The normal depth is re-established after a distance called backwater length.

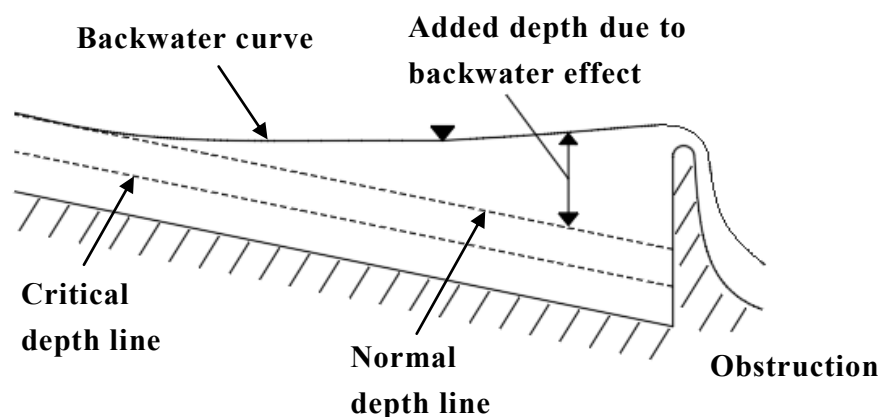


Figure 6 – Backwater profile in a subcritical flow

The basic idea of the use of a fictitious structure is the calculation of the discharge on the basis of the water level in two points, as suggested by the following formula (Meert *et al.*, 2016):

$$Q = f(h_1, h_2) \sqrt{2g(h_1 - h_2)} \quad (\text{Eq. 6})$$

Where $f(h_1, h_2)$ is a friction factor that can also be approximated as a function of the only downstream water level h_2 .

A different analysis is necessary for the calculation of the discharge in the reservoirs that are located in the transition zone (defined above). In this case two different formulas can be used, according to two different type of flow: the free or drowned flow conditions. The choice of the most appropriate formula is based on a threshold value that depends on the upstream water level, the downstream water level and a hypothetical weir.

The following figure is a scheme of all the above mentioned modules, including both the calculated values, i.e. Inflow (input value), Storage and Water Level (first input and then output values) and Discharge (output value), as well as the different types of calculations, according to the peculiar features of the river reach (lower boxes in the scheme).

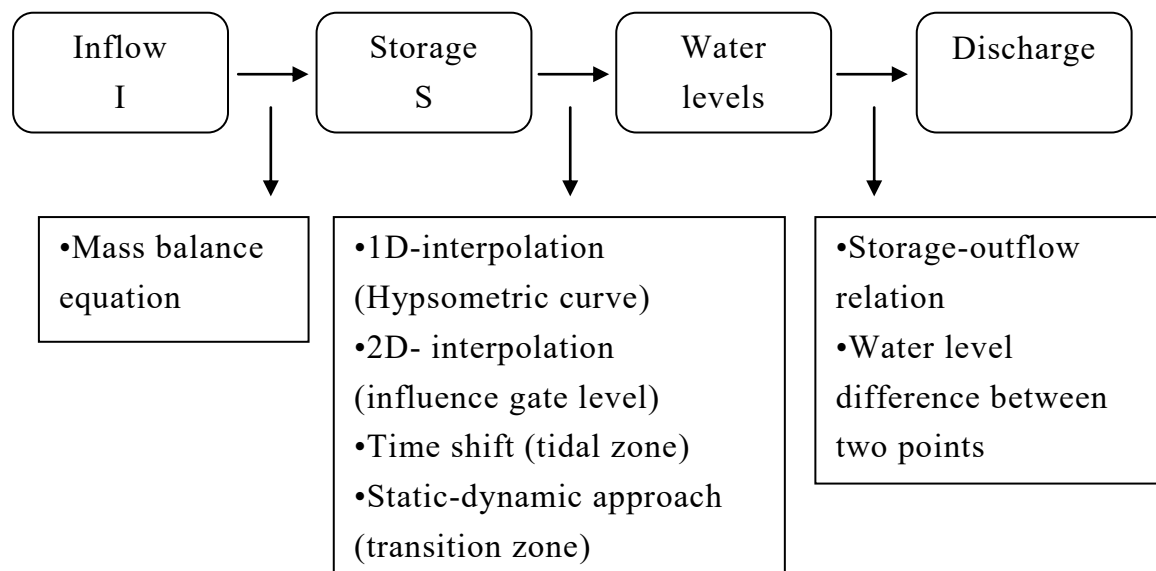


Figure 7 – Scheme of conceptual modelling approach

In the conceptual modelling approach, it is also possible to calculate three optional outputs: the gate levels, mean depths and mean velocities. The first one gives an estimation of the gate levels of the controllable hydraulic structures

that are located along the river. The second one differs from the calculation of the water depths just because in this case the river bed level is subtracted from the water depth. Hence, two possible calculations, that are similar to the previously described methods valid for the water depths, can be used, i.e. a simple 1D-interpolation or the 2D-interpolation (if necessary). The third extra modulus is calculated with the traditional formula:

$$U = \frac{Q}{A} \quad (\text{Eq. 7})$$

Where U is the current velocity. The mean velocity can be determined with two possible methods. The easiest one only requires the discharge value as input and is applicable if the river reach doesn't show significant backwater effects. In this case there is a distinct relation between the discharge and the current velocity, therefore the classic 1D-interpolation can calculate the mean velocity in all the nodes. Otherwise, for all those reaches where the assumption of negligible backwater effects is no longer valid, the calculation requires the info about both the discharge and the storage values as input. The last two modules, i.e. the mean depth and the mean velocity, can be particularly useful for assessing the water quality in rivers. They help to provide information about the concentrations of the major pollutants that cause water quality degradation. This means that conceptual models have the advantage of constructing an integrated catchment modelling (Meert *et al.*, 2016).

- **Conceptualization procedure**

When the detailed hydrodynamic model is replaced by the conceptual model, a conceptualization procedure is necessary (Meert *et al.*, 2016). This is an iterative procedure that consists of three steps:

- Conceptualization and schematization of the river network: the main river, its tributaries and the floodplains are divided into reaches with a certain length and a certain storage capacity. The choice of the boundaries of each reach depends on the presence of hydraulic structures, on the type of reach and on the desired accuracy. The shorter the reach is, the higher the accuracy will be, but also the higher the instability of the reservoirs will be. Wolfs *et al.* (2015) suggest some useful guidelines that can help the modeller with the choice of the length of a reach and with the definition of the elements that form the

boundaries of the reach. These boundaries are usually elements, such as hydraulic structures, that can considerably influence the flow and that can generate backwater effects. Smaller reservoirs should be considered when higher accuracy is needed.

- Calibration of the conceptual model components: since this step requires a large number of data, using the results of the full hydrodynamic model, such as the MIKE11 model, is often a good choice. This procedure is more accurate if the simulation results of extreme events are considered. The other MIKE11 files that are required for the calibration of conceptual models are the network file, cross-section file, boundary file and finally the time series of the boundary data.
- Integration, simulation and validation: a C++ script contains all the validated model structures and is executed in MATLAB.

During the execution of the conceptual model two different time steps are defined. An external time step is used to save the results and is usually higher than the internal time step. Common values are one hour or fifteen minutes and the boundary data are also provided with this external time step. On the other side the internal time step is used to solve the above mentioned storage equation. This value is usually not constant, since very small time steps are only necessary in case of significant discharges. On the contrary, in case of lower discharges, a higher time step can be chosen, in order to reduce the calculation time.

These three steps are repeated until a good agreement between the results of the conceptual model and the ones of the detailed model is found.

There are several formulas that can statistically compare these values. Meert *et al.* (2016) use two different formulas to validate the conceptual model. The first one is the classic root mean squared error (RMSE) formula, which is a measure of the differences between the results of the detailed model (indicated as $Y_{obs,i}$) and the conceptual model outputs ($Y_{pred,i}$):

$$RMSE = \sqrt{\frac{1}{n} \sum_{i=1}^n (Y_{obs,i} - Y_{pred,i})^2} \quad (\text{Eq. 8})$$

A second method to compare the results is by means of the formula proposed by Nash and Sutcliffe (1970) that defines the efficiency of a model R^2 , as a function of the index of disagreement F^2 and the initial variance, F_0^2 :

$$R^2 = 1 - \frac{F^2}{F_0^2} = 1 - \frac{\sum (q' - q)^2}{\sum (q - \bar{q})^2} \quad (\text{Eq. 9})$$

Where q and q' are respectively the observed and computed discharges (or water levels) and \bar{q} is the mean of the observed values. In this way it is possible to compare the results for a certain number of calculation nodes.

Also Wolfs *et al.* (2015) use a modular conceptual modelling approach that is computationally efficient, stable and that can also cope with backwater effects. This approach can include elements like hydraulic structures, floodplains and dike levels. They develop a semi-automated software tool that is able to facilitate the set-up of the conceptual models. This tool, named Conceptual Model Developer (CMD), can automate some time-demanding procedures that need to be done for the choice of the most appropriate model structure. It first requires the time series of flows, water levels and gate levels as well as additional parameters that should be collected from the detailed models. Then it reads the spreadsheet which contains the network topology (which is previously defined by the modeller). After gathering all the required data, the CMD software identifies and calibrates the model structure, for which a parameter set is proposed. Finally, a script assembles all the model elements and the boundary data are prepared in order to run the simulations in the MATLAB environment. This modular design in which the modeller is assisted by the software tool shows good results in terms of time reduction and model accuracy and can be therefore applied in case of real time flood forecasts.

The reduction of the calculation time due to the use of conceptual models plays a key role in real-time flood control, especially in those cases where multiple simulations need to be run. A further example of the application of these models is given by Van Den Zegel *et al.* (2014). Their research makes use of conceptual models during the identification of the optimal positions of adjustable weirs, whose main function is to minimize the flood damage. In this case the Model Predictive Control (MPC) technique, which determines the control variables in the river network by simulating the possible future scenarios, is combined with the Genetic Algorithm (GA), i.e. an algorithm that

is capable of generating semi-random series of gate levels. During the optimization process, a large number of gate levels needs to be considered and this can lead to a very long calculation time. Indeed, once the series of the gate levels are applied to the river model, the total damage is calculated and all these steps are repeated so that at the end the optimal positions of the weirs are selected. In this case, the conceptual models replaced the time consuming hydrodynamic model implemented in the InfoWorks-RS software, that is currently used by the flood forecasting system of the Flemish Environment Agency (VMM).

The combination of the MPC-GA technique with the faster conceptual models is also used by Vermuyten *et al.* (2014), who propose an improved algorithm and apply it again to the Demer basin in Belgium.

Case study of the river Dender

2.1 Description case study

The river Dender is located in Flanders, i.e. the northern portion of Belgium which is part of the Low Countries. This region has always been characterized by high potential from flooding due to both the facts that some areas are below the sea level and that there is a dense network of rivers (Baumann, 2016). Although several flood control systems were implemented in the past by the Flemish government, the existing dike and canal system showed an insufficient capacity during the flood event of 1998. Several municipalities were hit by the overflowing of the Demer, a river in the eastern part of Flanders. From that moment on, the government began developing a flood forecasting system to predict discharge hydrographs not only for the Demer, but also for the other rivers in Flanders that are prone to flood. A large amount of data about the riverbed and the riverbanks was collected, including information on infrastructures like bridges or locks. Moreover, cross-sections of the major rivers were measured about every 50 meters and then mapped.

One of the most flooded rivers in that area is the river Dender, which is a right tributary of the river Scheldt. Its two sources (Eastern Dender and Western Dender) meet in the town of Ath, in the Walloon Region, and from here on it flows northward for 65 km (Meert *et al.*, 2016). In the city of Dendermonde it issues in the Scheldt, whose tidal oscillations influence the Dender. The downstream part of the Dender basin is located in Flanders, in a surface of 708 km², while the upstream part is located in Wallonia, in a surface of 675 km². It is a navigable river, since it has been completely canalized, and several hydraulic structures influence its water level all along its length. The eight current hydraulic structures were installed in the 19th century (Meert *et al.* 2016-b) mainly to allow navigation and partly to avoid inundation, however they are not enough to cope with the peak discharges during flood events. For this reason most of these control structures are going to be renewed for years to come. The aim is also to make them automated instead of manually operated as they currently are (Meert *et al.* 2016-b). The official website of the project STAR-

FLOOD, i.e. “STrengthening And Redesigning European FLOOD risk practices”, funded by the European Union and carried out from 2012 to 2016, focuses on Geraardsbergen, a small city in the southern part of Flanders (almost at the border with Wallonia) and gives some extra information. Geraardsbergen consists of several municipalities, that were protected by dike infrastructure after the damages due to the flood event in 2003. However, in November 2010 an even more extreme event occurred, causing further damages in that area. Indeed, the calculated peak discharge according to the previous events was 85 m³/s, while in 2010 a peak discharge of 130 m³/s was recorded. The following figure shows the Dender basin and the main cities along the river. The dashed red line at the bottom represents the border between Flanders and Wallonia. The watercourse that comes from the South-West, flows through Netherlands and finally flows into the North Sea is the river Scheldt.

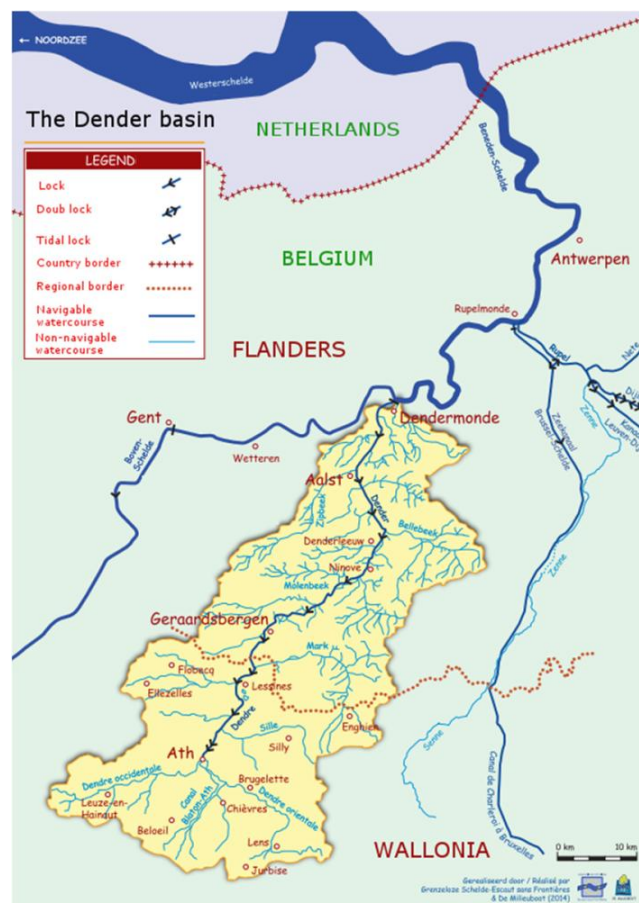


Figure 8 – Map of the Dender basin and main cities in the basin. (Source: Grenzeloze Schelde)

In the first part of this thesis the flood event occurred in June 2016 is considered. This event has been chosen because widespread flooding hit Belgium and this was due to continuous days of downpours and severe weather. During that period several rivers overflowed their banks and caused heavy damages to property. According to the portal of Global Disaster Alert and Coordination System (GDACS), the flooding was the worst that Belgium had seen in 50 years. Torrential rain approximately began in the late May/early June, hence the exact period that is simulated using the MIKE11 model goes from 20th May 2016 to 5th July 2016. The NAM model requires a set of model parameters, initial conditions and meteorological data for each catchment. Since NAM is a lumped model, this means that each catchment is described as a single value with a single rainfall input (Golasowski *et al.*, 2015). Twelve subcatchments have been considered for the Dender basin:

n.	ID	Area [km²]
1	410	19.05
2	411	55
3	420	51
4	421	49
5	422	88.4
6	423	15.56
7	430	28
8	4312	46.07
9	433	8
10	400	171
11	401	74
12	Wallonia	635

Table 1 – ID and areas of the catchments of the Dender basin

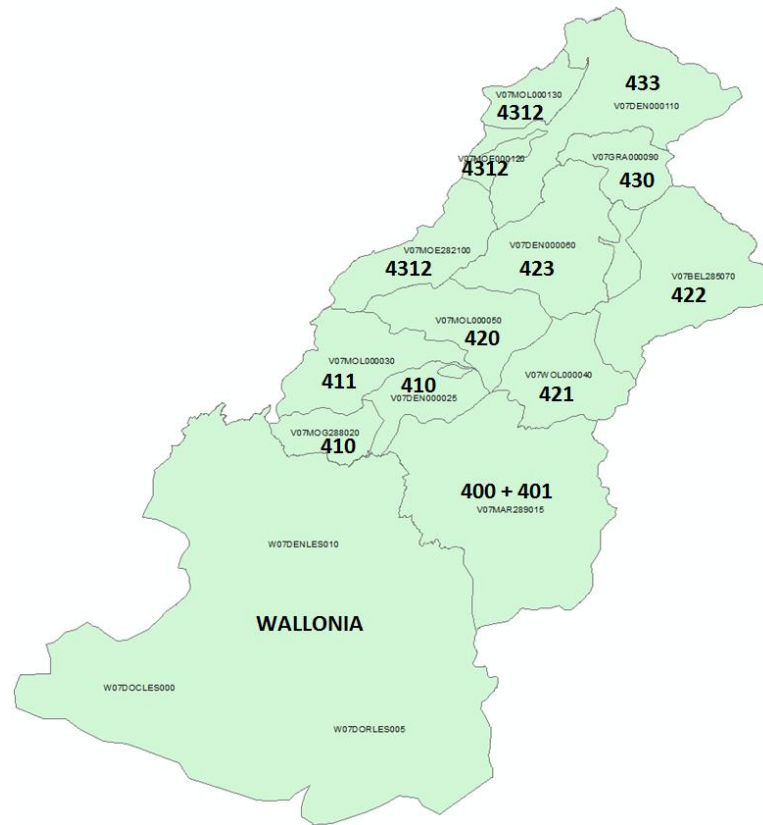


Figure 9 – Subcatchments of the Dender basin

The meteorological data required for the NAM model are:

1. Rainfall

The point source data are taken from the following gauge stations:

- Denderbelle (Station number: P07_022)
- Denderleeuw (Station number: plu05a-1066)
- Liedekerke (Station number: P07_006)
- Moerbeke (Station number: P07_021)
- Lessines, Bief Amont (Coordonnées Lambert x,y: 112294, 155703)

In this simulation, data from rainfall gauges, instead of radar data, are used, because of their higher accuracy. The first four stations from the list are located in Flanders, whereas the last station is located in Wallonia. A Time Series file is created for each station, where the rainfall is treated as accumulated volume, which means that the rainfall value at a specific time represents the rainfall volume since the last entered value (DHI, 2011). The more accurate the peak flow values are required, the finer the rainfall resolution is taken. It is also possible to specify variable time increments but this will not be considered for

this case study. The time step chosen for the rainfall Time Series used in this thesis is one hour.

2. Potential Evapotranspiration

Evapotranspiration data are taken from the station located in Liedekerke and a time step of one day has been considered sufficient. Also these data are treated as accumulated.

2.2 Results NAM model and comparison with observations

Figure 10 gives an overview of the rainfall-runoff discharges that are obtained with the NAM simulation.

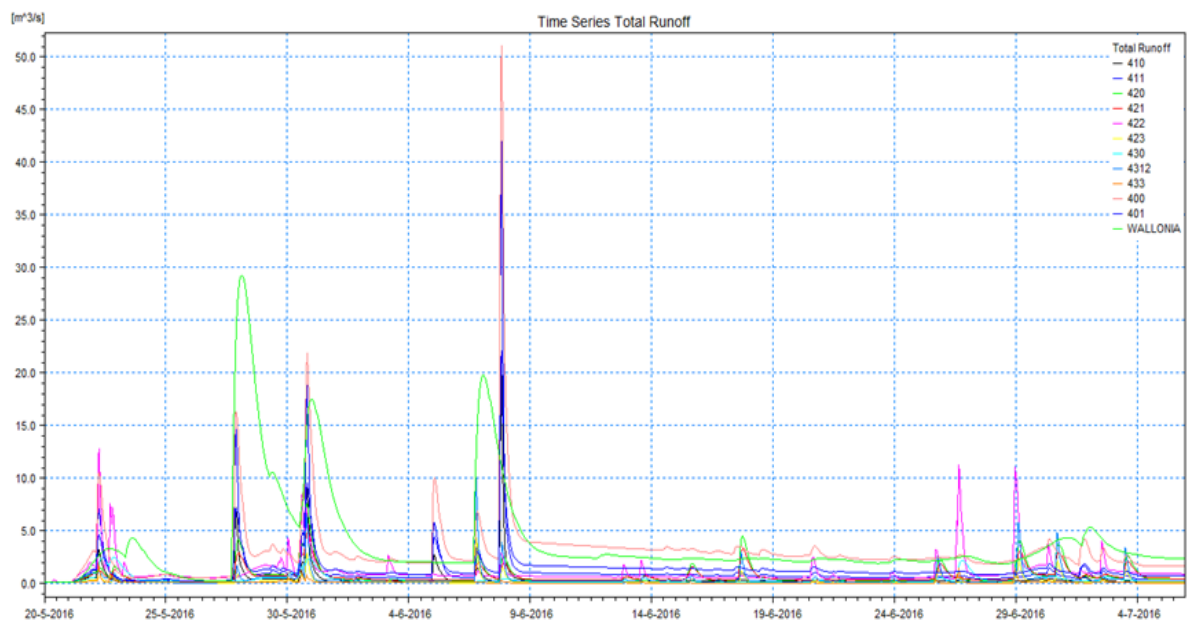


Figure 10 – NAM results

It is possible to compare the results from the NAM simulation with the actual measurements from www.waterinfo.be. The available measurement nodes on the tributaries of the river Dender are:

- Opwijk, Vondelbeek (Station number: L07_281)
- Essene, Bellebeek (Station number: L07_285)
- Aalst, Molenbeek (Station number: L07_28C)
- Iddergem, Molenbeek (Station number: L07_284)

The figure below shows the locations of the these four stations within the Dender basin.

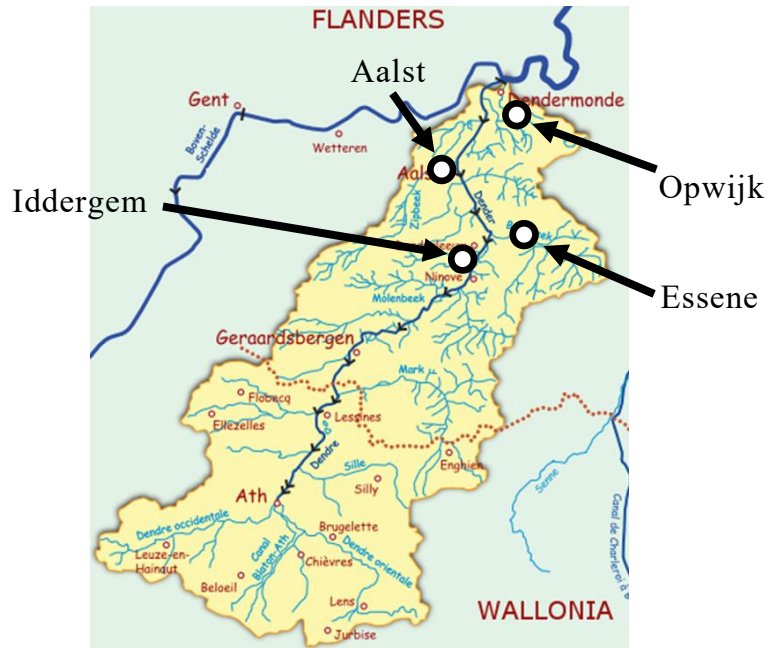


Figure 11 – Locations of the available measurement nodes

In the following figures the measurements downloaded from the *waterinfo* website are superimposed on the simulated values. The comparison can be visualized by plotting these data in Mike View.

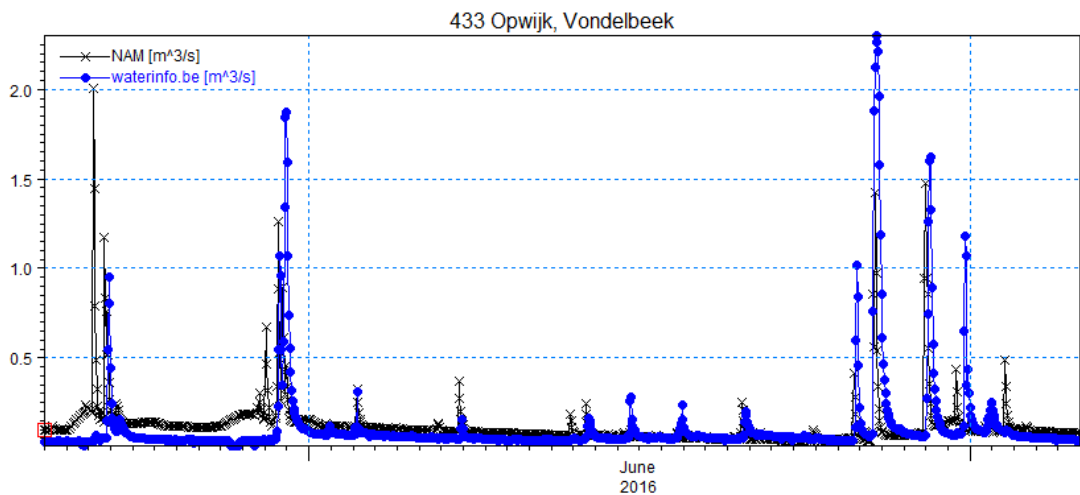


Figure 12 – Comparison: Opwijk, Vondelbeek

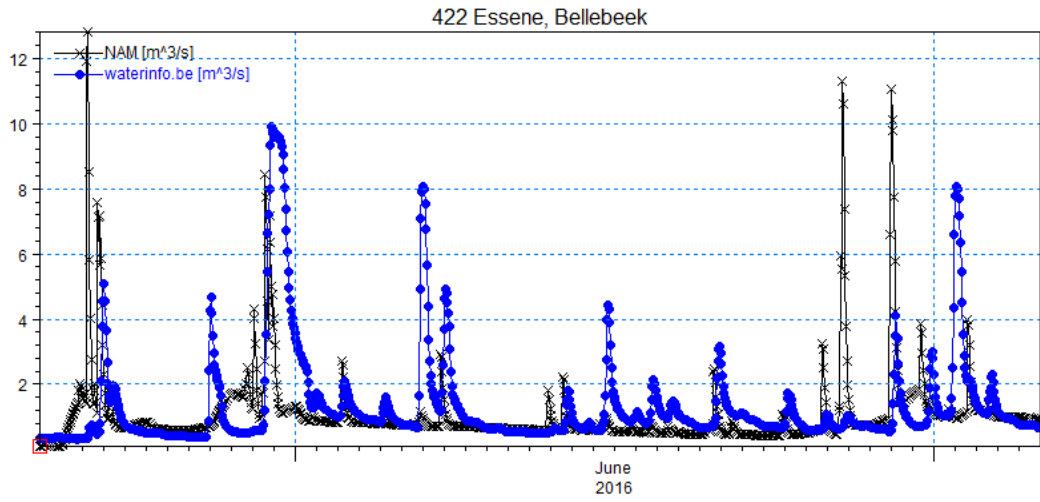


Figure 13 – Comparison: Essene, Bellebeek

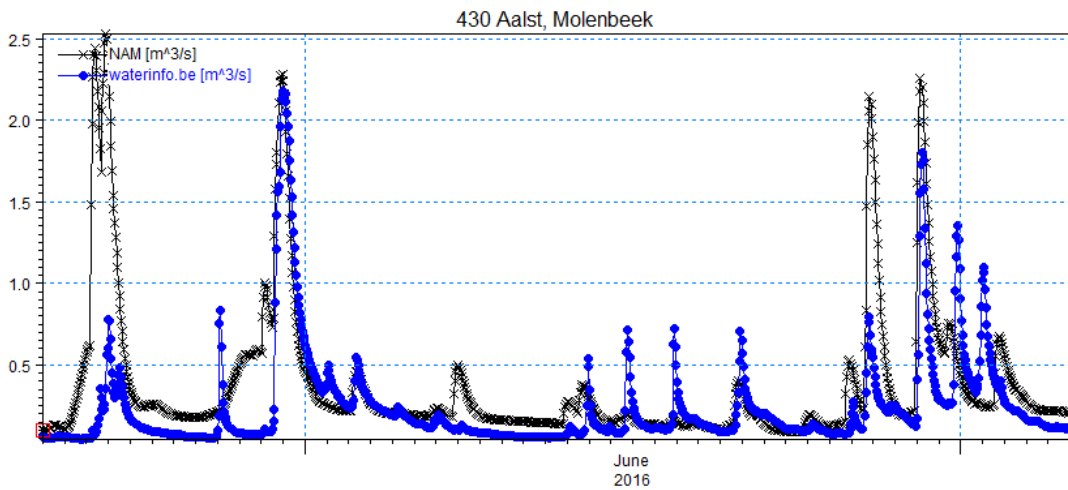


Figure 14 – Comparison: Aalst, Molenbeek

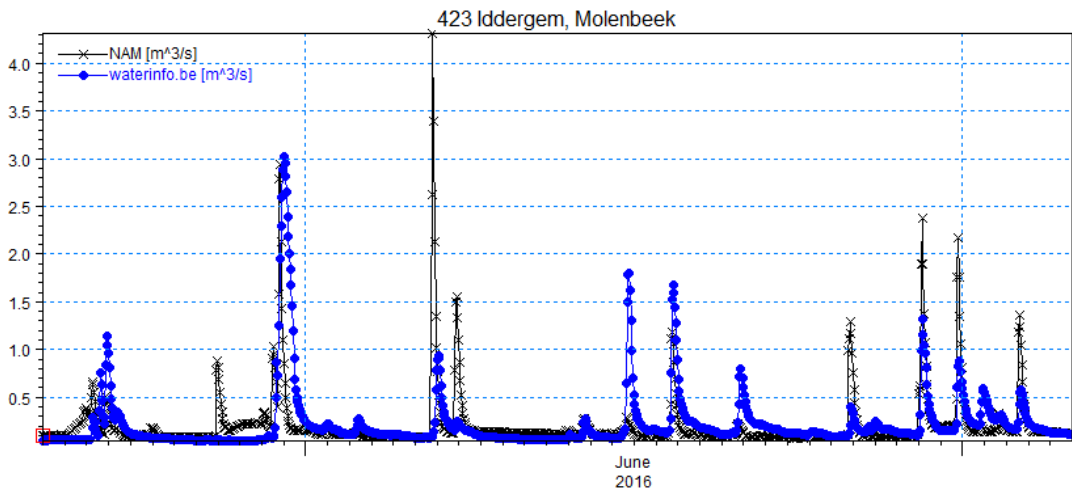


Figure 15 – Comparison: Iddergem, Molenbeek

It can be noticed that most of the peaks obtained with the NAM model match the ones from observations, however there are also some significant outliers visible in the graphs. There are multiple statistical parameters that can be used to compare the observed values with the simulated values. One of the mostly used parameters is the Nash-Sutcliffe efficiency, which was mentioned above in Eq. 9 and that compares the observed and simulated values at each time step. This value is 1 in case there is a perfect agreement between the simulation results and the observations, but a value higher than 0.3-0.4 is usually considered sufficient to state that the results are good. Moreover, the difference between simulated and observed values is also incorporated in the error matrices (which will be described in detail in Chapter 4, paragraph 4.1), so that if there is an error in the NAM results, the error matrices will try to reduce the average error. This means that in case a graph containing the simulated discharges (on the y-axis) and observed discharges (on the x-axis) is constructed, the ideal case of perfect agreement returns all points located on the bisector. In reality, this is hard to achieve and the comparison between the values will give a line with a certain deviation from the bisector, for example like the red line shown in Figure 16.

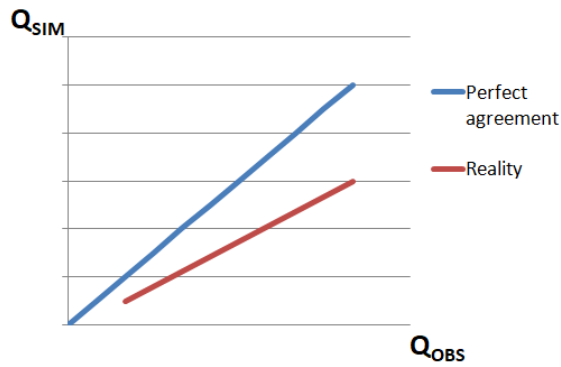


Figure 16 – Example of graph containing simulated and observed discharges in case of perfect agreement (blue line) and reality (red line)

When the error matrices are used, the red line moves closer to the blue one. In this way there is already a bias correction. Since in hydrology the input is not completely correct, accounting for the error is always advised to get more accurate results. Hence, the most convenient procedure consists of calculating the Nash-Sutcliffe efficiency and, in case the latter is smaller than a threshold value, accounting for the uncertainty. The problem of propagating the uncertainty through the model will be discussed in Chapter 4.

The graph below shows a real example of the graph in Figure 16, where observed and estimated discharges of catchment 430 are plotted. It can be noticed that, even if the trendline is not so far from the bisector, there is a great number of outliers, which means that discharges can be whether underestimated or overestimated.

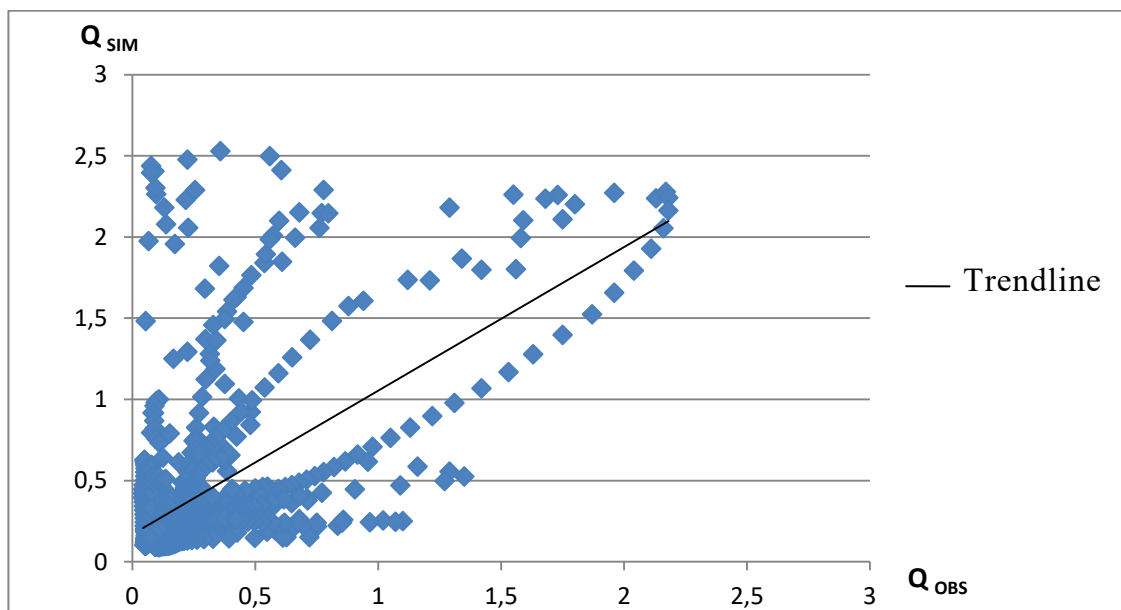


Figure 17 – Simulated and observed discharges for catchment 430 (Aalst, Molenbeek)

One last consideration about the NAM results is that in practice longer term simulations are considered, so that it is possible to see whether on average all the peaks are accounted for and whether there is any systematic overestimation or underestimation. However, this kind of analysis is not possible for the NAM simulation presented above, since a period of only one month and half has been considered. So the ideal simulation is when on average one gets all the peaks, but if one looks at one month this is quite uncommon because there are only two or three peaks. For instance this can be done for a period of one year.

2.3 River model results

2.3.1 MIKE11 results

For the simulation of the flood event of June 2016, the unsteady simulation mode is chosen for the hydrodynamic model implemented in the MIKE11 software. The input files required are:

- Network File

It requires the X and Y coordinates of the points located in the working area and the definition of the map projection (UTM, LONG/LAT etc.).

- Cross sections of the river Dender, its tributaries (Bellebeek, Mark, Molenbeek, Wolfputbeek) and the floodbranches that are implemented. Irregular, circular, rectangular or open section types can be selected. In this case, the latter is chosen, since this is the typical setting for river cross sections (DHI, 2011).

- Boundary data

Common boundary conditions are inflow and water level hydrographs, lateral flows along the river, specifications about possible structures. In this case:

- upstream boundary condition consists of NAM results from the catchment of Wallonia.
- downstream boundary condition consists of the water level in the river Scheldt.

The Scheldt has a tidal influence on the Dender and the measurement point is located in the city of Dendermonde.

- HD parameter

In this file it is possible to specify:

- Initial conditions: Water level and discharge.
- Bed resistance: The resistance formula may refer to the Manning “ n ” [$\text{s}/\text{m}^{1/3}$], Manning “ M ” [$\text{m}^{1/3}/\text{s}$], Chezy “ C ” [$\text{m}^{1/2}/\text{s}$] or Darcy-Weisbach “ k ” [m] coefficients. Here the Manning “ n ” description is chosen. The degree of roughness depends on several factors. In general, in open channel flow the main factors are surface roughness of the bed material, cross-section geometry, channel variations, obstruction to flow, type and density of vegetation and degree of channel meandering (Jarrett, 1985). In this case the range of “ n ” values goes from 0.025 [$\text{s}/\text{m}^{1/3}$] (used for smooth reaches of the river Dender) to 0.043 [$\text{s}/\text{m}^{1/3}$] (used for rough reaches).
- Flood plain resistance: this value is set to $n=0.1$ [$\text{s}/\text{m}^{1/3}$], that is the highest value in the model. This is reasonable since flood plain roughness is definitely higher than river roughness.
- Stratification: The number of layers in the stratified branches is 10. This number is assumed to be the same for all the stratified branches. Densities are calculated on the basis of the simulated water temperatures.
- Type of wave approximation
- Several additional parameters
- RR results from NAM simulation

The results of the hydrodynamic model are the water level and the discharge in the river Dender and its floodplains. These values are computed at each time step (as defined by the user). For this simulation a fixed time step of 1 minute is chosen. It is possible to check whether the event of June 2016 led to floodings or not. For this purpose the maximum water levels from the MIKE11 simulation and the dike levels of the Dender are compared.

Figure 18 and 19 show that floodings mainly occur at upstream areas (except for few downstream isolated points).

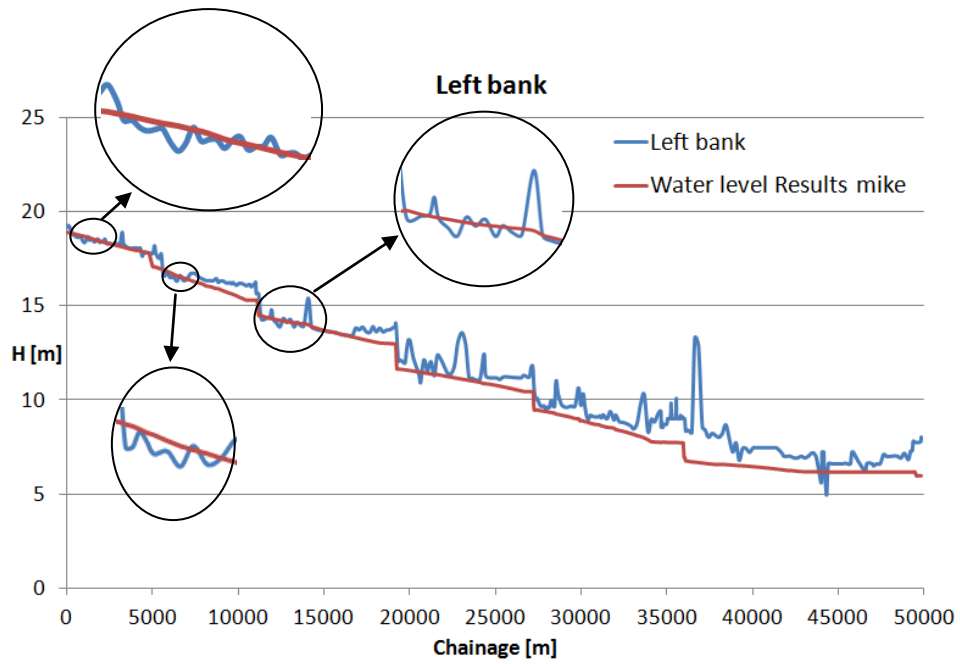


Figure 18 – Comparison: Left bank / water level (MIKE results)

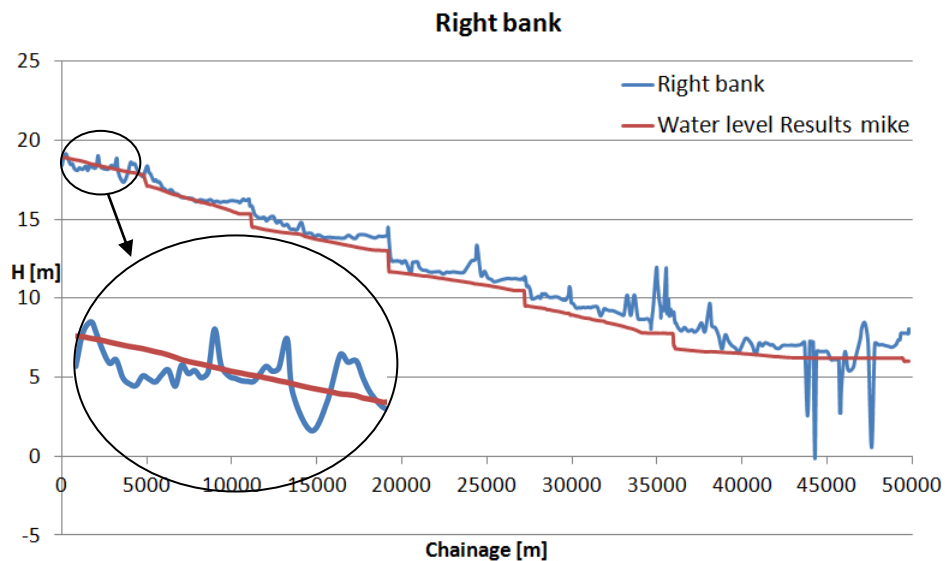


Figure 19 – Comparison: Right bank / water level (MIKE results)

MIKE11 can generate two-dimensional maps of water levels using the results of a quasi 2-D approach. Actually, MIKE11 always performs 1-D modelling, however a quasi two-dimensional approach can be obtained by modelling the floodplains as a network of fictitious river branches and spills (Willems *et al.* 2002). The branches represent the depressions in floodplains and the possible drainage canals, whereas the spills (or overflows) stand for topographical

elevations like embankments, roads, railways etc. The geometric data regarding branches and spills can be derived from the digital terrain model (DTM) in case this is available, and using a GIS system. The cross sections of the fictitious floodbranches are perpendicular to the axis of the main river and are supposed to be equal to the cross sections of the floodplains.

In order to produce a flood map, the output grid details need to be specified in the HD parameter file and the DEM input data for ground elevations are applied. For the generation of the following map a grid size of 4 m is chosen and a number of 500/800 cells for x/y direction, respectively, are set. This means that the map below is 2 x 3.2 km. Since from the comparison between the banks and water levels the upstream area is the most flood-prone, the mapping is limited to the area near Geraardsbergen (Figure 20).

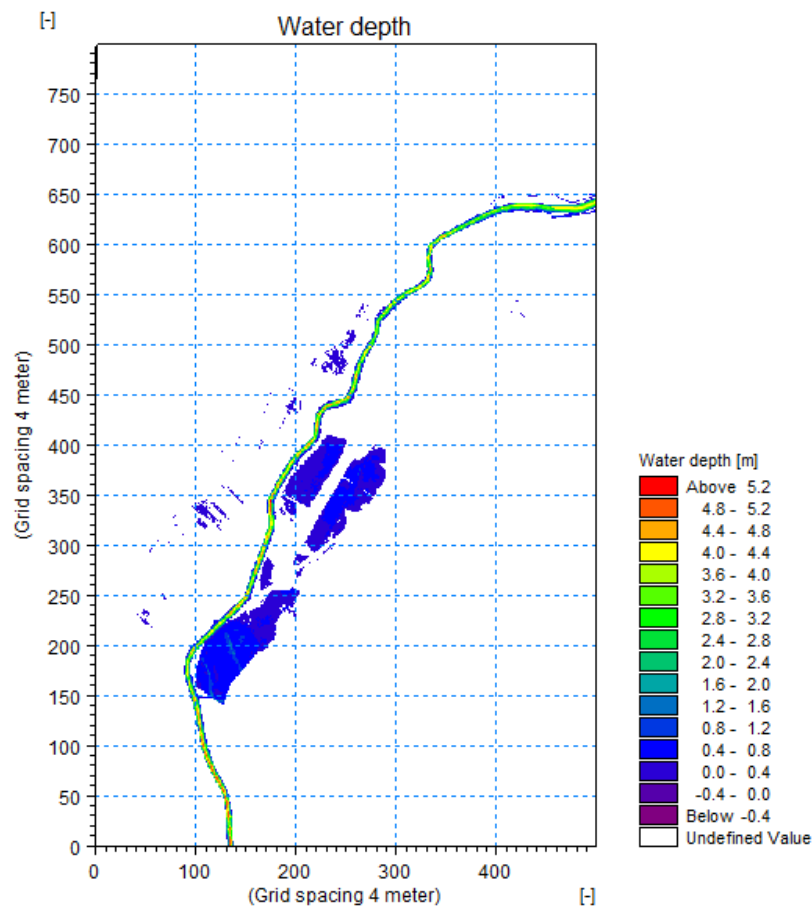


Figure 20 – Flood map near Geraardsbergen

While the results of the NAM simulation can be easily compared with the measurements available on the *waterinfo.be* website, it is not possible to check

the accuracy of the produced flood map. Indeed, the helicopter images for the flood event of June 2016 are not available yet.

Since for the MIKE11 simulation the area near Geraardsbergen has been selected on the basis of the results shown in Figure 18 and 19, it is useful to look at the time series of the discharge in Overboelare (a town comprised in the Geraardsbergen municipality). These values, which are available on the Flemish portal, show that the average discharge in Overboelare is very low (around 5 m³/s). However, the discharge can significantly increase during intense rainfall periods: it reached almost 120 m³/s during the extreme event of November 2010. This was the more extreme event in the last decade, but it was not the only one that led to flooding. Indeed, for this location flooding occurs whenever the discharge is greater than 55 m³/s and the following figure shows that there are a lot of peaks higher than this value.

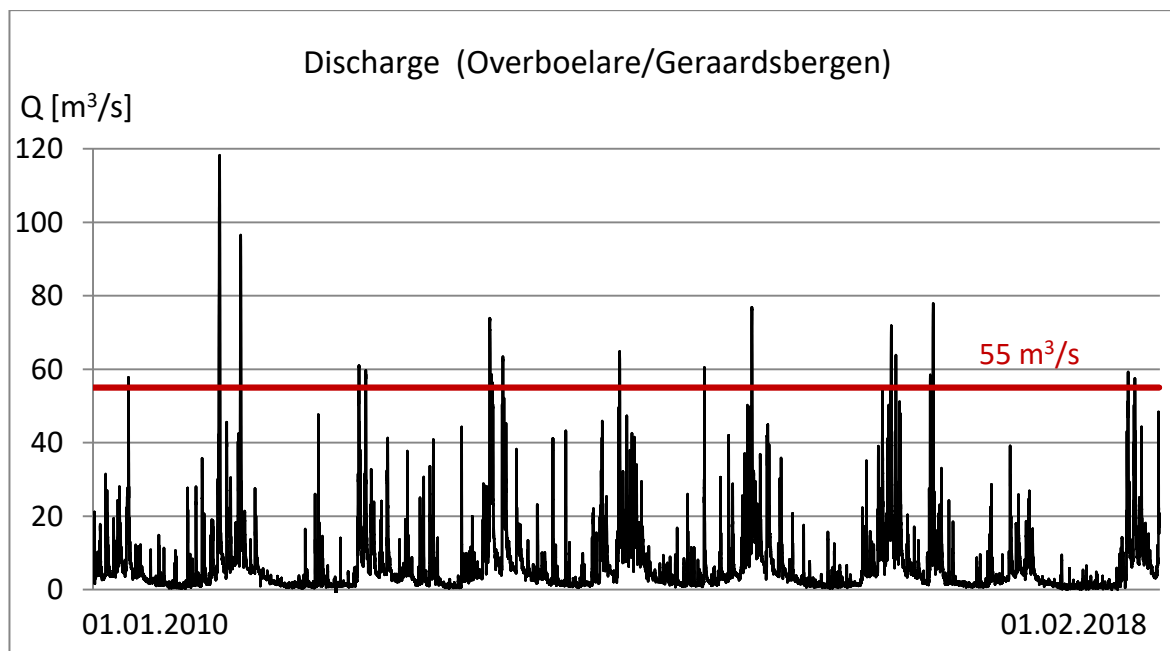


Figure 21 – Time series of the discharge in Overboelare (Geraardsbergen) from January 2010 to February 2018

2.3.2 Conceptual model results vs MIKE11 results

The schematization of the Dender network used in this thesis is the one proposed by Meert *et al.* (2016), where 82 reservoirs are defined: 20 to model the river Dender, 6 to model the tributaries and 56 to model the floodbranches (that are used to schematize the floodplains). Water level nodes, discharge nodes

and gate level nodes are located along the river and the floodbranches. A series of link channels are implemented to model the embankment between the river and the floodplains. As mentioned in Chapter 2, there are some guidelines that can be followed for the schematization of the river network. In this case the maximum length of one reach is 5961 m (used for the reach in the transition zone of the main river), while the minimum length is 90 m (used for one floodbranch). Table 4 in the appendix contains the delineation of the storage reservoirs that compose the conceptual model of the river Dender (Meert *et al.*, 2016). The construction of this conceptual model does not include the Walloon Region but only concerns Flanders. The input time series of the discharge refers to Lessines, a municipality in Wallonia close to the Flamish border.

In this thesis the results of the MIKE11 model and the conceptual model regarding two historical events (November 2010 and January 2011) are compared. The conceptual model used in the simulation includes all the current hydraulic structures in the Flemish Region (weirs, sluices and pumps).

The plots in Figure 22, 23, 24 show the water level in the river Dender in three locations:

- an upstream water level node, near Overboelare (chainage 3365), for which the easiest storage-water level relation is used to calculate the water level
- a water level node in the transition zone (chainage 39815), where the downstream tidal water level and the incoming discharge interact
- a downstream water level node situated in the tidal zone (chainage 45810)

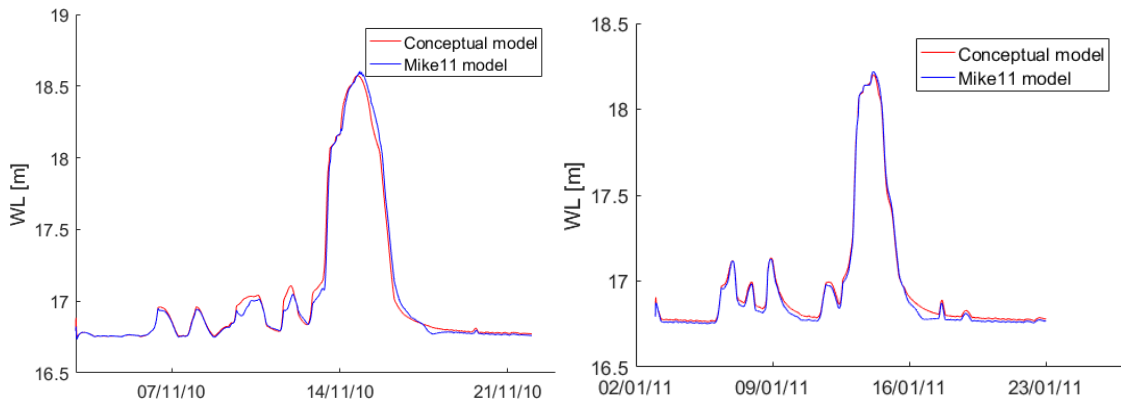


Figure 22 – Water level results of MIKE11 model and conceptual model (Left: November 2010, Right: January 2011), chainage: 3365

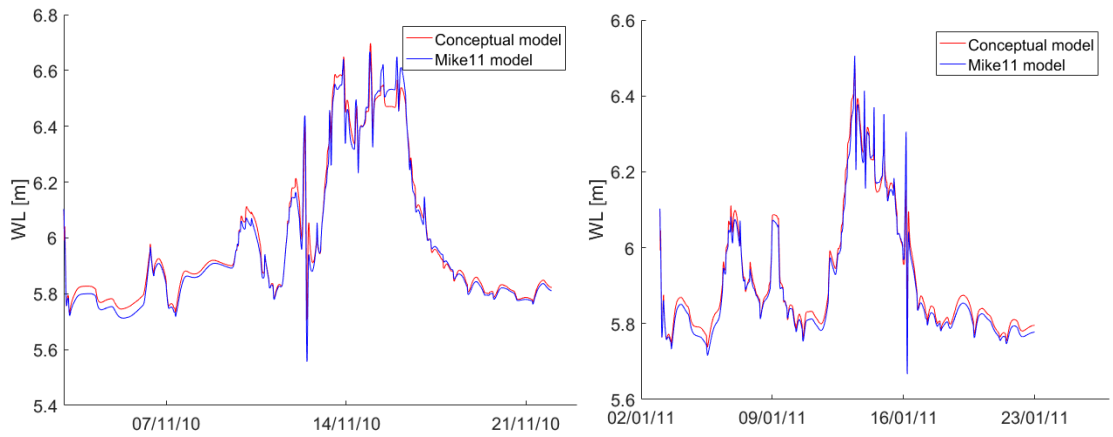


Figure 23 – Water level results of MIKE11 model and conceptual model (Left: November 2010, Right: January 2011), chainage: 39815, transition zone

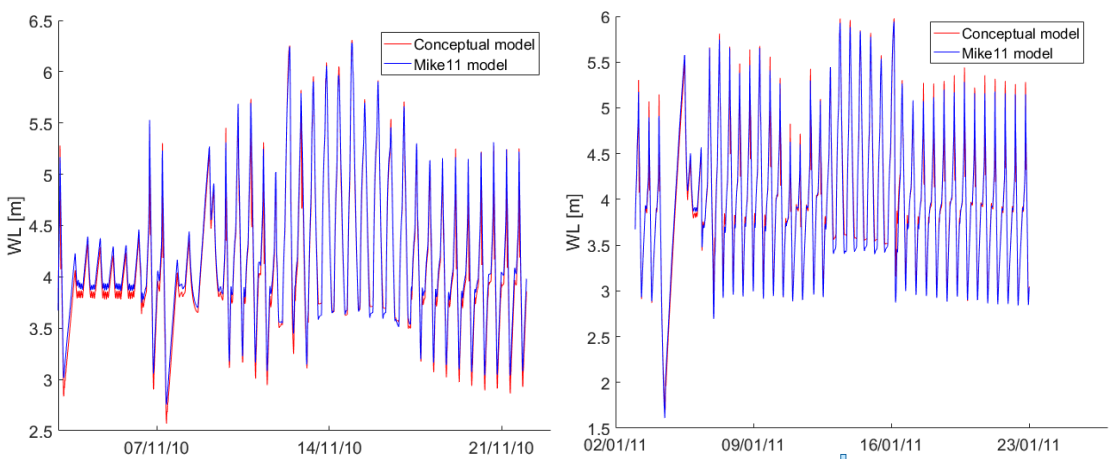


Figure 24 – Water level results of MIKE11 model and conceptual model (Left: November 2010, Right: January 2011), chainage: 45810, tidal zone

The graphs show that for both the events the differences of the water level between the detailed model and the conceptual model are very small. For each of the three locations (ordinary reach not influenced by backwater effects, transition zone and tidal zone) the order of magnitude of these differences is maximum few centimetres.

When the deviations are larger than a predefined value, the model schematization and components should be changed, as shown by Meert *et al.* (2016).

Uncertainty in river modelling

Flood forecasting systems are inherently affected by uncertainty. Indeed, each step of the flood forecasting modelling chain described in Chapter 1 has a certain degree of uncertainty. The sources of the uncertainty can be classified in three main groups and depend on different factors according to the hydrological or hydrodynamic model:

1. Input uncertainty

- *Hydrological model*: the prevalent sources of uncertainty are the rainfall and evapotranspiration estimations but also the use of different methods to interpolate punctual precipitation measurements (Thiessen polygons, inverse squared distance method, isohyetal method etc.).
- *Hydrodynamic model*: its uncertainty is mainly related to the total uncertainty that comes from the hydrological model results. There is also another important extra input uncertainty source in hydrodynamic river modelling, i.e. the tidal water levels in the downstream river. Indeed, in a flood forecasting application this information is not a priori known. For the case study of the river Dender this uncertainty is caused by the tidal variations in the river Scheldt. Since measurements have been used as downstream tidal boundary in this thesis, the uncertainties related to this component are rather small. However, they may become larger in case of forecasted water levels.

2. Parameter uncertainty

- *Hydrological model*: appropriate parameters values are not easy to identify and their uncertainty can be reduced by calibration. The uncertainty is also due to the fact that a limited number of parameters is used to model a complex process. Furthermore, they are subject to variability in space and time.
- *Hydrodynamic model*: there are uncertainties when specifying the cross sections, the topographical data, the Manning coefficient or in general the parameters that describe the river bed roughness or resistance.

3. Model structure uncertainty

- *Hydrological and hydrodynamic model*: there is an inherent uncertainty when the real world processes are approximated with simplified equations.

3.1 Uncertainty quantification

The traditional approach in hydrology is the deterministic forecasting. To be more exact, this is completely correct for the hydrodynamic component, for which only one simulation is run. In fact, in rainfall-runoff modelling, ensemble forecasts are usually considered, so that the results are actually not completely deterministic. In forecasting, where the objective is to make predictions for the next 2-3 days, input data are also predictions. For instance in Belgium, where the rainfall predictions are elaborated by the RMI, a number of rainfall patterns is considered (although without any indication about the likelihood of each prediction), in order to take into account different possible scenarios. However, the hydrodynamic model is run only once, since multiple simulations would take too long. Therefore it can be stated that deterministic results are usually considered in flood forecasting.

On the contrary, providing water managers information about uncertainty is recommended. Indeed it can help them to take founded decisions and it can increase the reliability of flood predictions. Montanari (2007) and Shrestha and Solomatine (2008) give an overview of the methods that were developed over the years to assess and quantify the uncertainty. They can be divided into six categories:

- *Analytical methods*: They calculate the exact probability distribution function making use of analytical derivations but are not commonly used because of the complexity of the models. They imply that statistical properties should be known.
- *Approximation methods*: Unlike the previous ones, these methods can even be applied to complex models. They provide the moment of the distribution of the output variables.
- *Simulation and sampling based methods*: They derive the output statistics by performing a Monte Carlo simulation. Golasowski *et al.* (2015) apply Monte Carlo method to estimate possible river discharge by modelling the rainfall forecast error. Random sampling of the input space is used to determine statistics of the model output. Time series of the input

precipitation data are created for each station. Once statistical properties are known, these random sets can be used as input parameters during simulations. Quantiles with specific probabilities p are selected from the Monte Carlo results and uncertainty hydrographs corresponding to specific probabilities are formed.

- Bayesian methods: They estimate and update the probability distribution function of the model parameters and then estimate the output uncertainty using Bayes' theorem. Beven and Binley (1992) introduced an alternative procedure based on these methods, the Generalized Likelihood Uncertainty Estimation (GLUE). However, the main problems of the GLUE are the large number of simulations needed (that makes this technique computationally demanding) and the subjective definition of the likelihood function. In order to have a higher efficiency, Blasone *et al.* (2008) recommends the use of the Markov Chain Monte Carlo (MCMC) scheme to sample the parameter space. This allows to take advantage of the flexibility due to the Monte Carlo analysis.
- Methods based on the analysis of the model errors: They analyze the model residuals and compare them with the observed historical data. One of the major drawbacks of these methods is that they make strong assumptions about the error distribution, i.e. homoscedasticity and normality, and this usually does not occur in reality. For this reason several methods have been developed, e.g. the Box-Cox transformation (Box and Cox, 1964). Willems (2009) applies the B-C transformation, whereby model residuals become independent of the flow value.

The transformation of the flow variable is performed as follows:

$$BC(q) = \frac{q^\lambda - 1}{\lambda} \quad (\text{Eq. 10})$$

where q is the variable and λ is the parameter that has to be calibrated.

Van der Waerden (1952) proposes the normal quantile transformation (NQT) in order to transform the cumulative distribution function to a Gaussian distribution. However, problems can arise when NQT is applied in flood forecasting systems due to small sample sizes. Bogner *et al.* (2012) propose a new method to solve this problem, making use of non-parametric regression methods and extreme value analysis.

- Fuzzy theory based methods: These are non-probabilistic methods that do not estimate the probability of the forecasted water levels and discharges, but they model the uncertainty associated with imprecision. When the temporal distribution of the precipitation is unknown, precipitation data are divided into subperiods in order to calculate the uncertainty. This method is used in case there is no information about the probabilistic forecast of precipitation.

Maskey *et al.* (2004) define “A” as a fuzzy set of X, if:

$$A = \{(x, \mu_A(x)), x \in X, \mu_A(x) \in [0,1]\}$$

Where $\mu_A(x)$ is the degree of belief that x is an element of A. They also give the definition of an α -cut of a fuzzy set A, i.e. the set of elements x for which A is larger than a predefined value α .

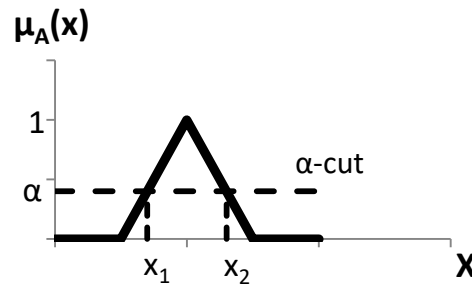


Figure 25 – α -cut of a fuzzy set

Huang *et al.* (2010) also used a fuzzy-based simulation method to deal with the multiple uncertainties related to the hydrological processes. They apply this method to the Tarim River Basin, China, an arid basin with limited water availability, for which the parameters uncertainty and interrelationship (e.g. uncertainties due to the geological properties of the area, to the interaction between surface and subsurface etc.) need to be taken into account in order to have a better water resources management.

Shrestha *et al.* (2006) propose a new method, the Uncertainty Estimation based on local Errors and Clustering (UNEEC), that is similar to the statistical approach but makes no assumptions about the distribution of the parameters and of the residuals. This method does not disaggregate the individual sources of uncertainties, like most of the statistical methods, but estimates the total model uncertainty by comparing the observed and modelled values. The first step consists in partitioning the input data into different clusters. Then the Prediction

Intervals, i.e. the intervals that correspond to a certain confidence level and that are defined by two quantiles, are computed for each cluster by fitting the empirical error distribution.

An example of a data-based approach that does not require any assumptions about the statistical properties, like the UNEEC, is the one designed by Van Steenbergen *et al.* (2012) and Van Steenbergen and Willems (2014), that was then used by Meert *et al.* (2017). This approach calculates the model residuals and considers absolute or relative differences between the observed data and the model results. The absolute model residuals for water levels are defined as follows:

$$e_{WL,i} = WL_{obs,i} - WL_{sim,i} \quad (\text{Eq. 11})$$

Where $e_{WL,i}$ is the model residual, $WL_{obs,i}$ is the observed water level and $WL_{sim,i}$ is the simulated water level.

On the other hand, relative model residuals are calculated for the discharges, to avoid an excessive increase of the value of the model residual that there would be with the absolute ones:

$$e_{Q,i} = \frac{Q_{obs,i} - Q_{sim,i}}{Q_{sim,i}} \quad (\text{Eq. 12})$$

Where $e_{Q,i}$ is the model residual, $Q_{obs,i}$ is the observed discharge and $Q_{sim,i}$ is the simulated discharge.

After the partition of the model residuals into clusters, an empirical cumulative distribution function is calculated for each cluster and a two-dimensional matrix is constructed. In Table 2 a 14×21 matrix for the catchment of Viaene is shown. Each column corresponds to a given percentile (0, 0.05, 0.10 ... 0.95, 1) while each row corresponds to a certain model output. In the example below the model output that is considered is the discharge. The values in the matrix indicate the error values, e :

Q\Perc	0	0,05	0,10	0,15	0,20	0,25	...	0,95	1
0	-0,552	-0,135	0,130	0,222	0,292	0,375	...	3,347	4,022
0,11	-0,552	-0,135	0,130	0,222	0,292	0,375	...	3,347	4,022
0,24	-0,561	-0,454	-0,398	-0,335	-0,265	-0,229	...	1,189	1,976
0,40	-0,860	-0,703	-0,624	-0,563	-0,524	-0,498	...	0,088	0,326
0,66	-0,886	-0,783	-0,741	-0,711	-0,687	-0,664	...	-0,050	0,235
1,08	-0,915	-0,859	-0,825	-0,800	-0,781	-0,761	...	0,241	0,813
1,68	-0,920	-0,887	-0,861	-0,832	-0,810	-0,782	...	0,613	1,083
2,43	-0,922	-0,870	-0,822	-0,782	-0,739	-0,697	...	0,684	1,104
3,44	-0,924	-0,841	-0,738	-0,641	-0,572	-0,494	...	0,661	1,145
4,74	-0,915	-0,756	-0,603	-0,483	-0,410	-0,329	...	1,122	1,837
6,81	-0,845	-0,590	-0,459	-0,408	-0,345	-0,276	...	0,868	1,187
9,15	-0,634	-0,451	-0,379	-0,311	-0,263	-0,201	...	0,600	0,829
13,02	-0,641	-0,506	-0,397	-0,351	-0,312	-0,295	...	0,206	0,441
20,14	-0,641	-0,506	-0,397	-0,351	-0,312	-0,295	...	0,206	0,441

Table 2 – Two-dimensional error matrix

It is therefore possible to construct confidence intervals around the simulated values, according to Meert *et al.* (2017). Their width is calculated as follows:

$$WL_{CF,i} = WL_{sim,i} + e_i \quad (\text{Eq. 13})$$

$$Q_{CF,i} = Q_{sim,i}(1 + e_i) \quad (\text{Eq. 14})$$

Where $WL_{CF,i}$ and $Q_{CF,i}$ are respectively the water level and the discharge that constitute the confidence intervals.

In Figure 26 the model residuals for the catchment of Viaene are plotted as a function of the simulated discharge. Their variance is higher for lower water levels, whereas after a certain value of the discharge, the errors become constant. This is due to the definition of relative model residual that has been considered in this analysis. The different values of the percentiles can give both an overestimation (i.e. negative model residuals) or an underestimation (i.e. positive model residuals) of the discharge.

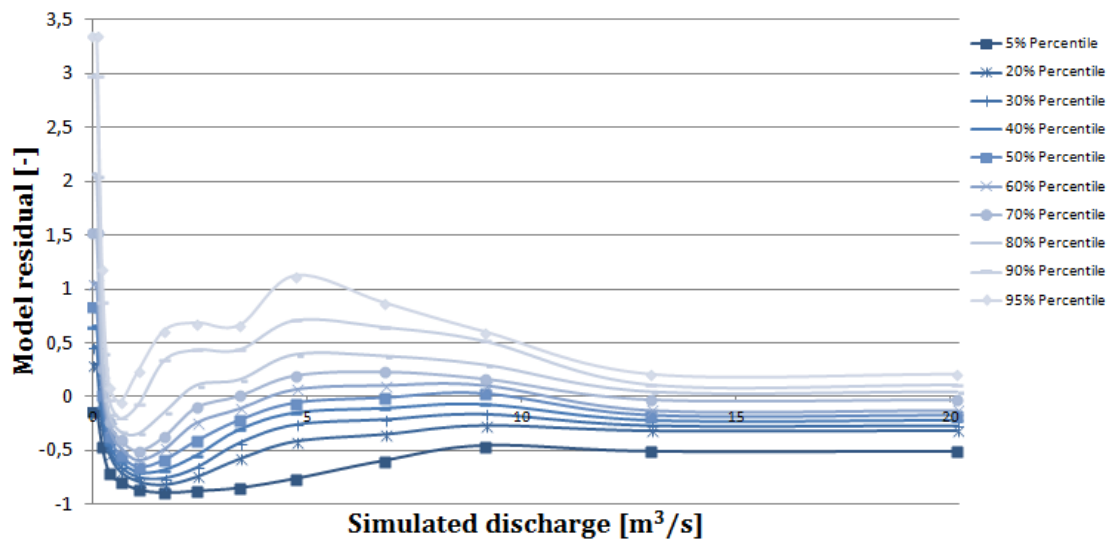


Figure 26 – Errors versus simulated water levels (catchment Viaene)

The non parametric data-based approach used here is described in detail by Van Steenberg *et al.* (2012), whose aim is to provide probabilistic water level forecasts. However in the latter case, a three-dimensional error matrix is built, where the error is a function of the percentile, of the forecasted water level (indeed the residuals are higher for higher water levels) as well as of the time horizon of the forecast (the forecasts are more accurate for closer time horizons). After the construction of confidence intervals, the method was compared to the Bayesian approach and it finally showed more reliable confidence intervals, especially when a bias correction was applied to the maximum predicted water level. It was also a useful tool for calculating the exceedance probabilities of alarm levels, evaluated by analyzing the values of the Correct Alarm Ratio and the Miss Rate.

3.2 Propagating uncertainty through model

The data-based approach considered in the previous paragraph quantifies the total model uncertainty. Then the uncertainty can be propagated through the model and this allows to know the effect of the uncertainties on the simulated water levels and on the simulated flood maps. An alternative method is to propagate the input and parameter uncertainties separately, in such a way that the contribution of each source of uncertainty can be identified. In the latter method a sensitivity analysis is conducted and the contribution of the model uncertainty can also be quantified as the difference between the total model

uncertainty and the sum of the input and parameter uncertainty (Meert *et al.*, 2017).

Another example of sensitivity analysis is the one performed by Brandimarte & Di Baldassarre (2012). In this case only the two main sources of uncertainty were considered, i.e. the inflow and the model parameters. Then a large number of simulations was run and uncertain flood profiles, instead of deterministic flood profiles, were generated. The aim of this novel method is to include the uncertainty information when designing flood profiles, since the use of a constant freeboard in the traditional approach usually underestimates the uncertainty. The flood profiles corresponding to certain percentile values (5th, 50th and 95th) are plotted first taking into account only the model parameter uncertainty and then taking into account only the design flood uncertainty.

There are many sources of uncertainty and each of them influences the simulated outputs. Researchers can opt either to consider a large number of sources or to focus on just one source and then see its impact on final results. For instance, the study by Jung and Merwade (2011) investigates the uncertainty arising from the following three variables: discharge, topography and Manning's roughness coefficient n . For each variable a probability distribution is created and then Monte Carlo simulations are run using the random values picked from the aforementioned distributions. The probability distribution for discharge is based on historic peak flows, while random DEM are generated by assuming a uniform distribution in order to take into account the uncertainty on topography. Finally, another uniform distribution is assumed for Manning's n values, which are different according to the type of land use.

The example that is proposed in this thesis takes the upstream boundary from Wallonia (Qin) as boundary for which the uncertainty will be propagated. Then the effect of the uncertainty on this boundary is assessed. A vector of ten equally spaced points between 0.05 and 0.95 is chosen; these ten intervals produce ten new time series (Qnew) that can be used as upstream boundary. For the uncertainty propagation considered in this section, the conceptual river model presented in Chapter 2 is used, because of its lower calculation time.

Table 3 shows the Matlab commands used to generate the new time series: these values are found by means of the interpolation table containing the errors, as described in the previous paragraph. It can be noticed that the intervals of the

incoming discharge from Wallonia are expressed in $\text{m}^3/\text{s}/\text{km}^2$ and then multiplied by the area of the catchment.

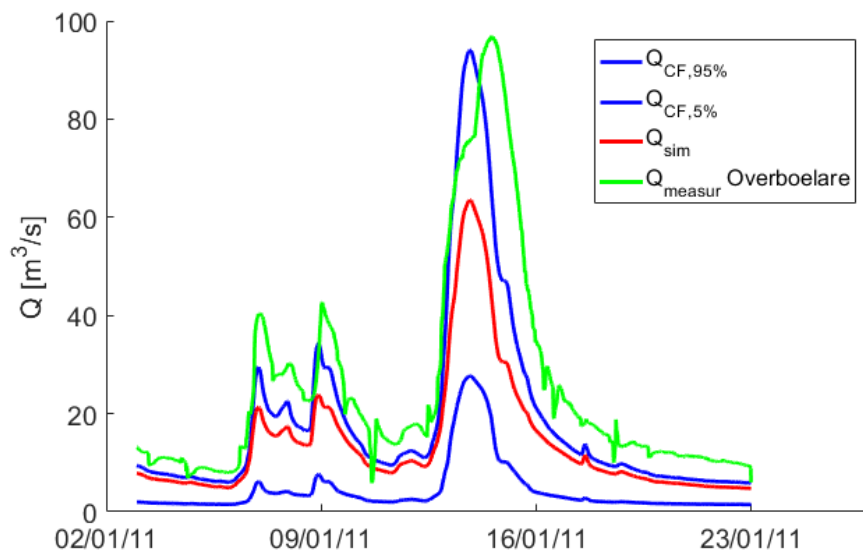
```

errors = linspace(0.05, 0.95, 10);
for j = 1:10
    Qnew(:,j) = (1 +
        interp2(CI_NAM.Wallonia.Intervals_Area*Area,
            CI_NAM.Wallonia.Perc,
            CI_NAM.Wallonia.CDF',Qin,errors(j)))' .* Qin;
end

```

Table 3 – Matlab commands for construction of confidence intervals

Once the upstream boundary is propagated through the model, the results are collected. The plots in Figure 27 show respectively a) the value of the incoming discharge after the construction of confidence intervals, b) the water level at one location (chainage 3365 of the river Dender) and c) the water level in one of the floodbranches (in this case floodbranch4_1_274). In the first two graphs the 95th and 5th percentiles delimit the 90% confidence interval, while in the third graph all the ten percentiles are plotted. The width of the confidence intervals is calculated by means of equations 13 and 14. A further comparison is made by plotting the discharge and water level measurements at the station of Overboelare (for the floodbranches no measurements can obviously be used).



a)

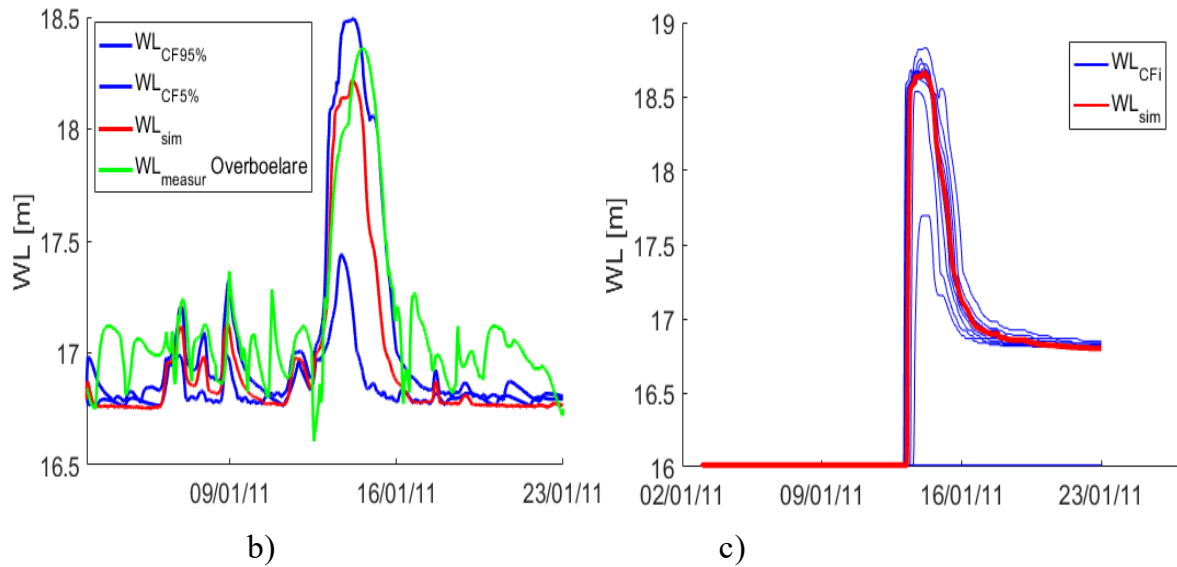


Figure 27 – a) Confidence intervals of upstream boundary, b) Water level results in the Dender and c) Water level results in a floodbranch

There are some remarks that can be made about the differences between the measurements and the model outputs. Graph a) shows that the simulated discharge is slightly underestimated for the lower discharges, while the peak value of the measured discharge is very close to the 95% percentile. This is due to the way the propagation of the uncertainty is done. Indeed, the amount of the uncertainty on the input is based on the maximum value of the event (here the event of January 2011), that is in this case $63 \text{ m}^3/\text{s}$. While in reality the magnitude of the error is proportional to the discharge value, in the uncertainty propagation it is assumed to be a constant value for all time steps. Independent events are first identified and the maximum peaks of the time series of simulated water levels and discharges are selected for each event, according to the Peak Over Threshold (POT) algorithm (Willems, 2009). In this way the serial dependence of model residuals in time can be neglected (Meert, 2017). Indeed each model residual corresponds to a certain POT. This means that the error magnitude is just a function of the maximum value in that event and of course of the percentile. Thus, since only one value is selected for each event, the input discharges are multiplied by the same factor. However, errors in lower discharges are not relevant when one focuses on the maximum values.

The second remark concerns the water level differences in graph b), which affect again the lower discharges. These differences are reasonable since there are usually some extra uncertainty sources, that are even more visible for the water levels. This can be explained by the control structure that is present in

Geraardsbergen. Indeed, the actual structure consists of a number of beams that regulates the opening of the gate. The gate level changes depending on the number of beams and this influences the water level. In reality the regulation of the beams is done manually, therefore it is rather impractical to change them every hour. On the contrary, the model changes the gate level every time step of the calculation with much smaller increments. However, the more interesting value is again the maximum water level and the graph b) shows that it totally falls in the confidence interval.

Finally, in graph c) it can be noticed that, as expected, the value of the water level in the floodbranch is zero until the inundation of the floodplain occurs.

Probabilistic flood mapping

4.1 Methodology

The previous sections have shown that each step of flood modelling is affected by a certain degree of uncertainty due to input, parameter and model structure uncertainty that involve both the hydrological and the hydrodynamic model. As a consequence, the generation of potential flood maps in flood forecasting can lead to results that are not completely correct. For this reason during the last years the scientific community highlighted the necessity of developing flood maps that are could take into account the inherent uncertainty of the modelling process, although some authors argue that neglecting the estimation of uncertainty in hydrological and hydraulic modelling is beneficial (Pappenberger and Beven, 2006). Several studies show that the adoption of probabilistic flood maps (PFMs) is advised during the choice of mitigation measures and strategies in flood management.

The use of PFMs is also extremely important in dike-protected reaches, where a potential dike failure can be an additional source of uncertainty. Domeneghetti *et al.* (2013) focus on the uncertainty that comes from upstream boundary conditions, downstream boundary conditions and possible dike failures and then construct PFMs. For this purpose they use the Inundation Hazard Assessment Model (IHAM), i.e. a probabilistic-deterministic model that is capable of taking into account the failure mechanisms involving the dike (overtopping, piping and micro-instability). The IHAM model solves a 1-D model relative to the river and the zone between dikes, then considers a dike breach module to assess the stability of the dike and finally uses a 2-D model to simulate the flooding in the floodplains after the dike breach. This model is particularly useful in flood hazard estimation, where both natural (or aleatory) and epistemic sources of uncertainty are present. The former is due to the natural variability of the phenomena, while the latter is also called the “knowledge” uncertainty. This incomplete knowledge involves model uncertainties as well as statistical uncertainties caused by small samples and observation error (Hall and Solomatine, 2008). Apel *et al.* (2005) list the epistemic sources of uncertainties such as error in model selection, selection of data, partial series, selection of

distribution function, variability estimation of levee parameters. Uncertainties involve every step of the flood hazard mapping. First of all, the hydrological analysis is affected by measurement errors, incorrect estimation of parameters and peak discharge, incorrect hydrographs as well as insufficient length of time series. Also the construction of the rating curves (often used as downstream boundary conditions) is not completely correct because for instance the river geometry has been considered constant over time (while significant variations occur in reality). Another parameter that changes in space and time is the roughness coefficient, whose variability can considerably influence the flood dynamics (the uncertainty in the calibration of effective roughness parameters has been amply investigated by Pappenberger *et al.*, 2005).

The importance of visualising the uncertainty through PFMs in river flood forecasting is also highlighted by Van Steenbergen (2014). In his study, an uncertainty analysis is first performed, then different quantiles of water levels are calculated, finally the water levels in the floodplains corresponding to the given quantiles are calculated. The flood probability can be therefore computed by comparing the quantiles of the water levels in the floodplains and the digital terrain model data.

Since PFMs are produced in case of possible extreme flood conditions, the time to run multiple simulations is very limited. Thus Van Steenbergen (2014) uses conceptual models to reduce the calculation time which would be otherwise too long if a large amount of simulations are run using the detailed hydrodynamic models (like MIKE11 and InfoWorks-RS).

Alfonso *et al.* (2016) propose a novel methodology where the concept of Value of Information (VOI), originally developed in economics and defined as the amount a decision maker is willing to invest in acquiring information (Bouma *et al.*, 2009) is applied. In this method the PFMs provide the information about the uncertainty in order to construct VOI maps. Indeed, there are two types of flood map that can be produced for the estimation of the flood extent. The first one consists of the most common deterministic flood maps, i.e. binary maps that define two states of floodplains: flooded and dry areas. In this case unit values are associated with wet cells (indicated in Figure 28a with probability of flooding $P(w)=1$), while zero values are associated with dry cells ($P(w)=0$). When this type of maps is used, there isn't any complicated decision-making process for water managers, who just have to execute the emergency

plan or apply the predefined strategy in case the flood is expected. The message that they receive is clear, though it can be completely wrong.

On the contrary, probabilistic flood maps are an indication of the degree of certitude of floodplain inundation (Alfonso *et al.*, 2016). In these maps the likelihood of flooding is expressed by a certain probability $0 \leq P(w) \leq 1$, as shown in Figure 28b. Therefore, the agent makes a choice that takes into account the information about the uncertainty related to that flood event.

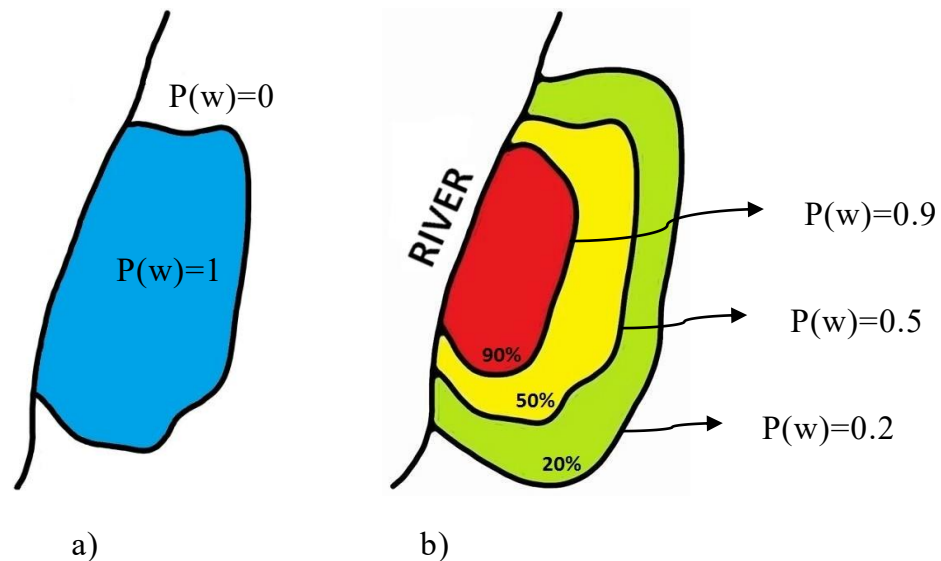


Figure 28 – a) Deterministic and b) probabilistic flood map

The procedure suggested by Alfonso *et al.* (2016) allows the decision-maker to choose among actions, relying on the uncertain flood hazard information provided by PFMs. The first step is therefore the production of PFMs, which represent the prior belief that the agent has about a potential flood event. These maps are obtained using flood inundations models together with historical flood data and then running Monte Carlo simulations that take into account the hydrological uncertainty. The result is the above mentioned map composed of cells with a certain probability of flooding $P(w)$.

The second step is the construction of a decision map in order to change the land use during spatial planning. This map helps understand whether a certain choice (e.g. urbanization or not of a flood-prone area) is correct. Considering the binary decision map, the choice of urbanizing that area is taken in case the probability of flooding is lower than a threshold value ρ , otherwise the decision map will suggest to not urbanize the area.

The third step consists of assessing the likelihood of the flood map by means of a matrix that indicates whether the message “ m ” about the inundation status “ s ” of a certain area is reliable or not. The matrix that expresses the likelihood $P(m|s)$ of receiving this message depends on the following parameters:

- R_0 and R_1 , i.e. dry and wet cells respectively;
- D_1 and D_0 , i.e. urbanized or not urbanized cells respectively.

In other words:

$$P(m|s) = \begin{bmatrix} \alpha(R_1 \cap D_0) & \alpha(R_1 \cap D_1) \\ \alpha(R_0 \cap D_0) & \alpha(R_0 \cap D_1) \end{bmatrix}$$

The flood map has a perfect quality when $P(m|s) = \begin{bmatrix} 1 & 0 \\ 0 & 1 \end{bmatrix}$, that means that the wet cells of the obtained flood maps exactly correspond to the flooded areas in the reality.

In the fourth step the consequences of different choices are evaluated and this is done by considering the possible scenarios that follow the different actions. The consequence matrix is determined by the combination of two decisions (e.g. either to change the land use or not) and two status (e.g. either flood occurs or not). Each of these four cases entails a certain outcome.

Finally, a VOI map based on the steps described above is generated and high values of the map mean that additional information is required in order to make a choice.

This methodology is a good example of application of PFMs in flood hazard estimation and the case study of Barcelonnette, in the South of France, shows that it can be a very useful tool during the decision-making process.

4.2 Source of uncertainty of the case study: incoming discharge from Wallonia

Several sources of uncertainty can affect the accuracy of flood maps. The main classification identifies the input, parameter and model structure uncertainty as the three main classes in which the uncertainty is traditionally subdivided. Then each study can focus on a different variable or on a group of variables. For instance, as mentioned in paragraph 3.2, Jung and Merwade (2011) consider the uncertainty arising from discharge, topography and Manning’s n . The type of hydraulic modelling, hydrologic modelling and terrain

analysis also plays a great role in the uncertainty quantification because different modelling approaches can lead to slightly different results.

In this thesis the upstream boundary from Wallonia (Q_{IN}) is selected as boundary for which the uncertainty will be propagated. Hence, the incoming discharge from Wallonia is the parameter that needs to be changed to produce the lines that define the probabilistic contour plots. By varying this factor it is possible to quantify the effect of the uncertainty on the discharge and then visualize it by means of PFMs. However, this is not the only source of uncertainty that can be considered for the model in question. For example, the tidal water level in the river Scheldt represents another significant source of uncertainty for the hydrodynamic river model, since it is not a priori known in a forecasting application. In this thesis the choice of the incoming discharge from Wallonia is due to the fact that this information is probably less accurate than the downstream boundary condition. Indeed, since 1980, water management in Belgium has been devolved to the three regions of Flanders, Wallonia and Brussels Capital Region (Flemish Environment Agency, 2012). The regional water authorities then inform the central federal government about the current situation and the government decides whether to recognise the flood event as a disaster or not. Hence, the flood forecasting and warning systems between the regions are not uniform: the data collected from the surrounding regions are produced with completely different models and there is no information about the associated uncertainty. Moreover, it is possible that data are not communicated reliably between the forecast centres. For this reason, the discharge from Wallonia has been selected for the uncertainty propagation phase of this case study, even if in general different sources can be considered. The more numerous the considered uncertainty sources are, the more reliable the conclusions about uncertainty estimation and confidence intervals will be.

As mentioned in paragraph 3.1, the uncertainty estimation was conducted by using the data-based approach designed by Van Steenbergen *et al.* (2012), where the forecast residuals (as defined by Eq. 11 and Eq. 12) represent the differences between historical observed data and simulated data. The residuals are subdivided into different clusters, since their values depend on the magnitude of the simulated discharge. An empirical cumulative distribution is constructed for each cluster. Such statistical analysis leads to the production of two dimensional error matrices which contain the percentile values of the residuals, as shown by

Table 2 in Chapter 3. In this way there is not a unique and deterministic value of the incoming discharge, but a probability distribution calculated on the basis of the comparison between historical measurements and predictions. Note that, for the case study in question, one specific historical event is considered (January 2011), hence observed discharge measurements are in theory available. However, the aim of PFMs production is to forecast future scenarios. In case of future predictions, the incoming discharge cannot definitely be measured, but it is the result of a previous modelling itself. This means that it includes all the input, parameter and model structure uncertainties of the upstream catchment. In this case it is the catchment of the Wallonia, since the boundary condition considered for the case study is the discharge from Wallonia.

4.3 Results

In this thesis PFMs are produced making use of the conceptual models in order to calculate the quantiles of water levels in the floodplains. The flood event considered for the production of PFMs is the one occurred in January 2011. All the necessary steps are executed in the MATLAB environment. First of all, the conceptual model is run so that the time series of the water level corresponding to that event can be computed. The most likely flooded areas in the Dender basin are identified. This can be easily done by comparing the maximum water levels (obtained running the conceptual model) with the cross section data stored in the MIKE11 files. It turns out that the most upstream river reach in the Flemish Region is the most likely to flood, i.e. the reach between the south of Geraardsbergen to Ninove. After that, the reservoir numbers corresponding to the area one is interested in, need to be identified in the conceptual model delineated in the appendix.

For the production of the first PFM, reservoirs 1 and 2 for the river Dender and reservoirs from 27 to 37 for the floodbranches are considered. The resulting PFM shows the flooded area at the south of Geraardsbergen that corresponds to FLOODBRANCH4_1, FLOODBRANCH4_2, FLOODBRANCH4_3, FLOODBRANCH4_4 and FB_R_8. The second PFM refers to the zone between Geraardsbergen and Ninove and corresponds to reservoir 7 for the river Dender and reservoirs 46, 47, 48, 49, 52 for FLOODBRANCH2_1, FLOODBRANCH2_2, FLOODBRANCH2_4 and FLOODBRANCH2_5.

After simulating the conceptual model, all the necessary data regarding the locations of the nodes are collected and processed. The exact correspondence between the water level nodes of the selected reservoirs and their corresponding X,Y coordinates is found. The values of the maximum water level in these nodes are saved.

Then the digital elevation model (DEM) is loaded, while another raster containing all the maximum water levels is constructed. The nearest-neighbour interpolation is used to calculate the water level raster. By using this method one assumes that the water level for a given cell (point A in the figure below) is equal to the water level in the closest point where the information is available (point B). Indeed the location of point B depends on the location of the water level nodes implemented in the conceptual model.

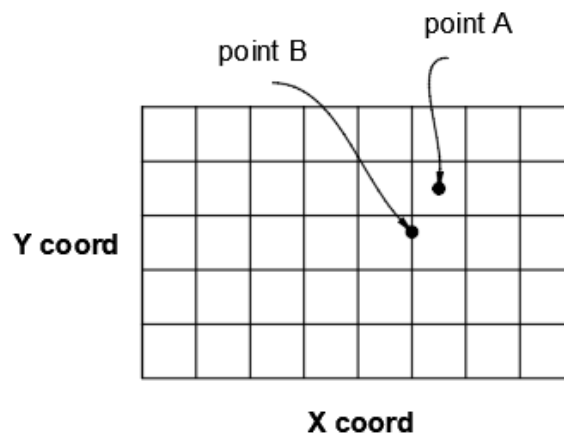


Figure 29 – Nearest-neighbour interpolation used in flood raster

The shortest distance between the DEM coordinate and the coordinate of the water level node is given by the formula:

$$d = \sqrt{(X_{DEM} - X_{WL_NODE})^2 + (Y_{DEM} - Y_{WL_NODE})^2} \quad (\text{Eq. 15})$$

Finally a flood raster can be constructed by making the difference between the maximum water levels and the DEM values. Negative values are disregarded or set to zero and they correspond to dry areas, whereas positive values indicate that the floodplains are flooded. The figure below shows an example of cross-section extended onto the floodplain. According to the procedure described above, the maximum water level among all the water level values at different time steps of a given event is selected. If a certain location corresponds to a DEM value that is smaller than the calculated WL_{max} , this point is flooded. The aim of the simulations in this part of the thesis is to find the probability of

flooding, which is the ratio of the number of simulations that led to flooding and the total number of simulations $\left(\frac{\#sim}{\#tot\ sim}\right)$. In the example below and for a given flood event, different water level values are obtained because the uncertainty propagation has led to different incoming discharges. For instance, if the incoming discharge from Wallonia is $50\ m^3/s$, the maximum water level for the cross-section at a certain chainage is $WL_{max,1}$. Instead, if the discharge is $100\ m^3/s$, this gives a different water level, which is for example $WL_{max,2}$. Hence, assuming that the PFM is generated taking into account these two simulations, this means that the probability of flooding is 100% for location no.1 because both the simulations lead to flooding. On the other side, location “n” is not always flooded, but it has a probability of 50%, indeed one simulation indicates flood and the other one does not.

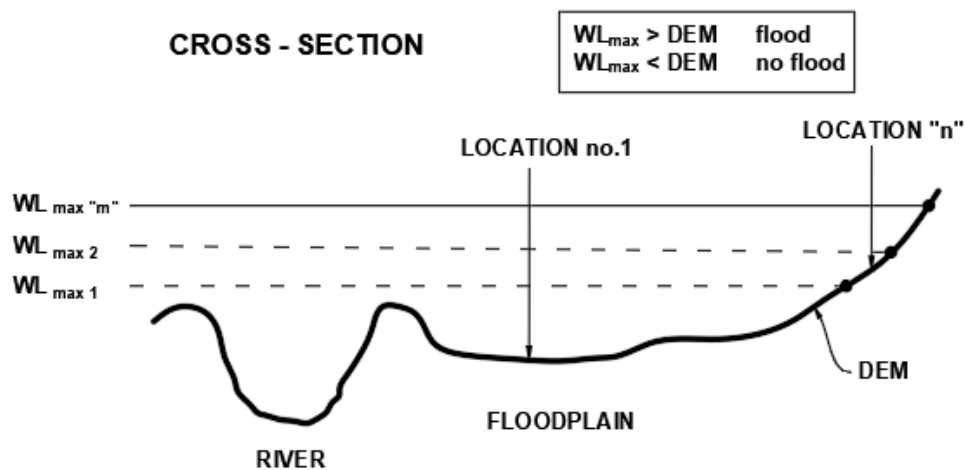


Figure 30 – Identification and comparison between water level and DEM values at a given location

In the following figure the locations of the produced PFMs are shown in the Dender basin.

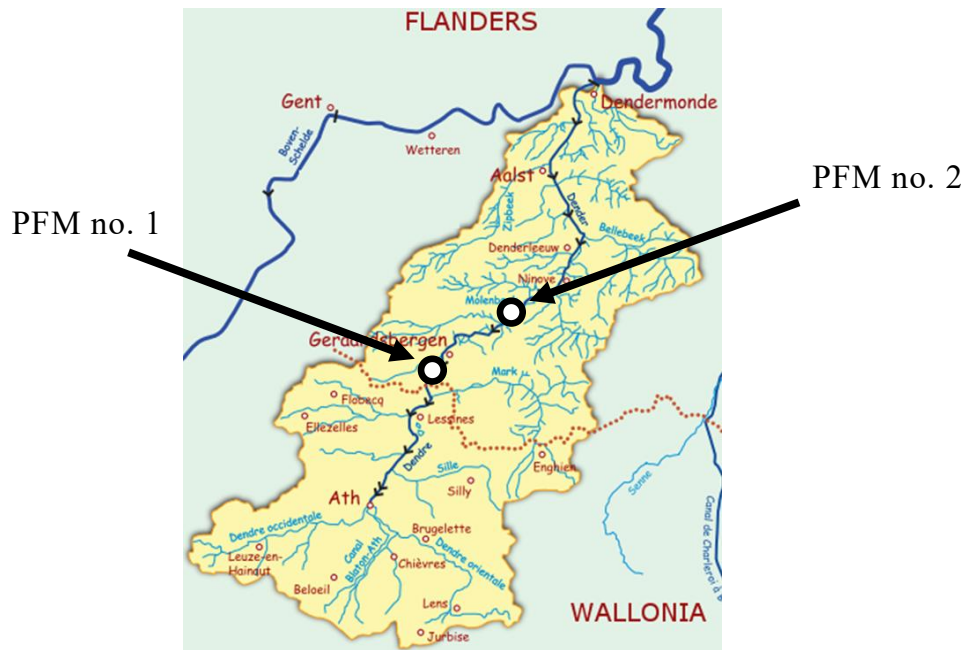


Figure 31 – Locations of the produced PFMs

In this thesis twenty intervals are considered for the uncertainty propagation of the upstream boundary from Wallonia during the simulation of the conceptual model. Indeed the number of intervals in Table 3 is increased from 10 to 20, in order to obtain higher resolution. This means that the confidence intervals are defined by the following vector:

[0.025 0.075 0.125 0.175 0.225 0.275 0.325 0.375 0.425 0.475 0.525 0.575 0.625 0.675 0.725 0.775 0.825 0.875 0.925 0.975]

The procedure adopted to achieve PFMs consists of two main steps. The first one is the generation of twenty different rasters (that correspond to the twenty confidence intervals). These rasters only contain zero and one values, which means that, for each simulation, each cell is identified as flooded or not. Once multiple rasters are produced, they are combined and the probability of flooding is computed. The final probability raster does not consist of 0-1 values, but consists of percentage values.

Figure 32 and 33 show PFMs obtained with the above mentioned procedure, where the white colour means that the probability of that area to be flooded during the event of January 2011 is 0%, while green, yellow and then red colours indicate progressively higher probabilities of that area to be flooded.

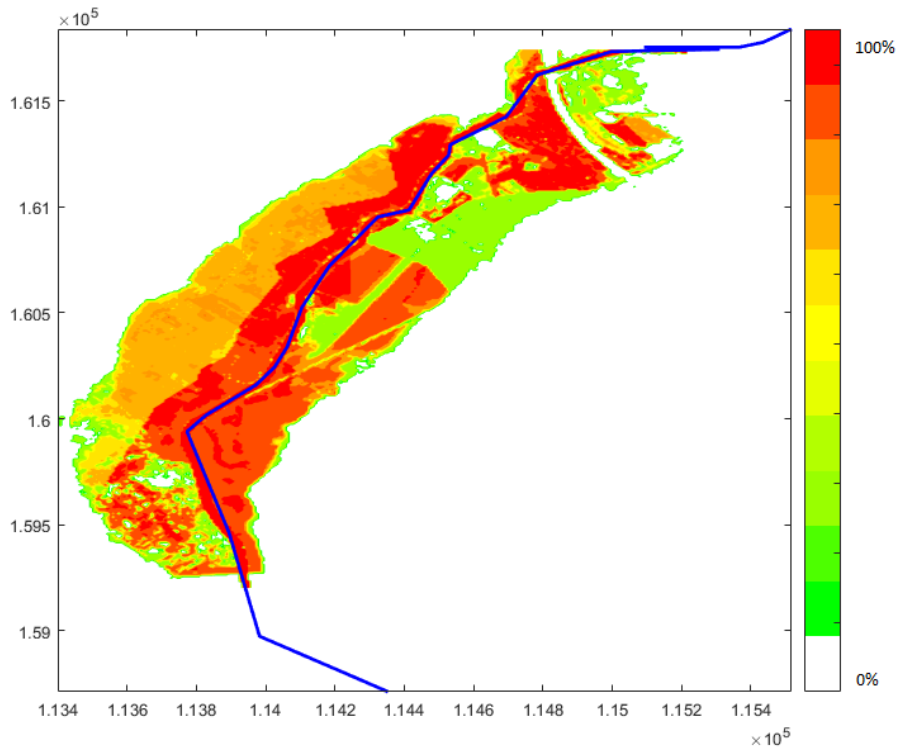


Figure 32 – PFM of the area at the south of Geraardsbergen (flood event of January 2011)

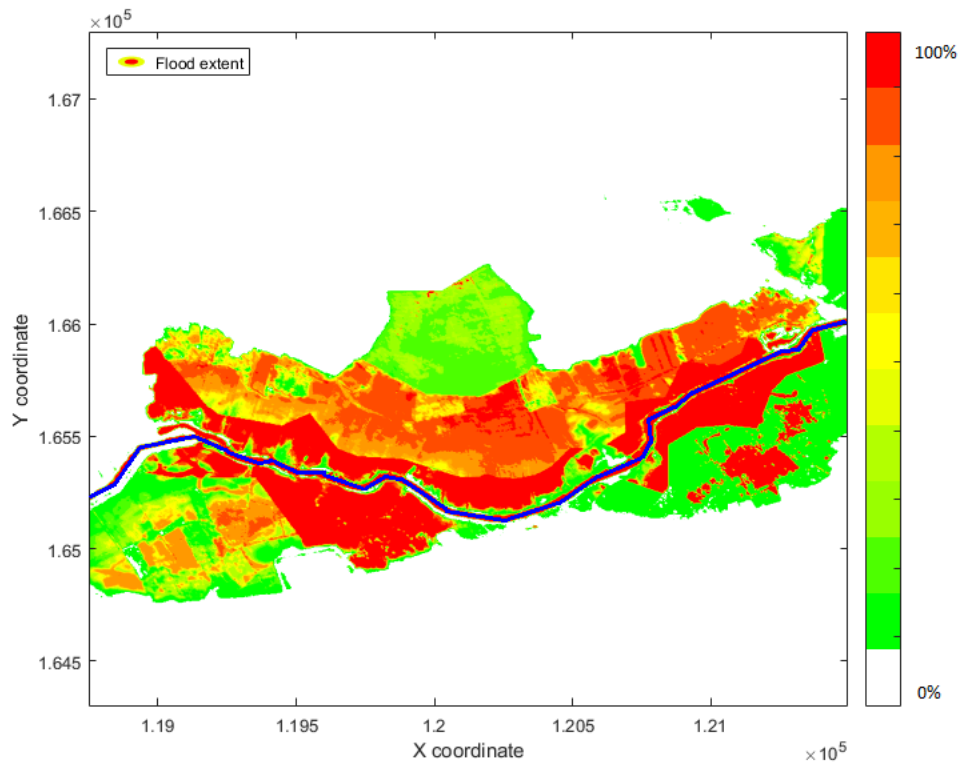


Figure 33 - PFM of the area between Geraardsbergen and Ninove (flood event of January 2011)

It can be noticed that the flood extents shown by the two PFM's above are quite similar to the maps obtained using helicopter images in Figure 34 and 35, even though the latter refer more generally to the recent flooded areas of the last twenty years. These are the so-called ROG maps and are based on manual cartography, photographs, (areal) movies, local terrain knowledge and other data collected/produced by water authorities, municipalities and provinces (Source: European Commission).

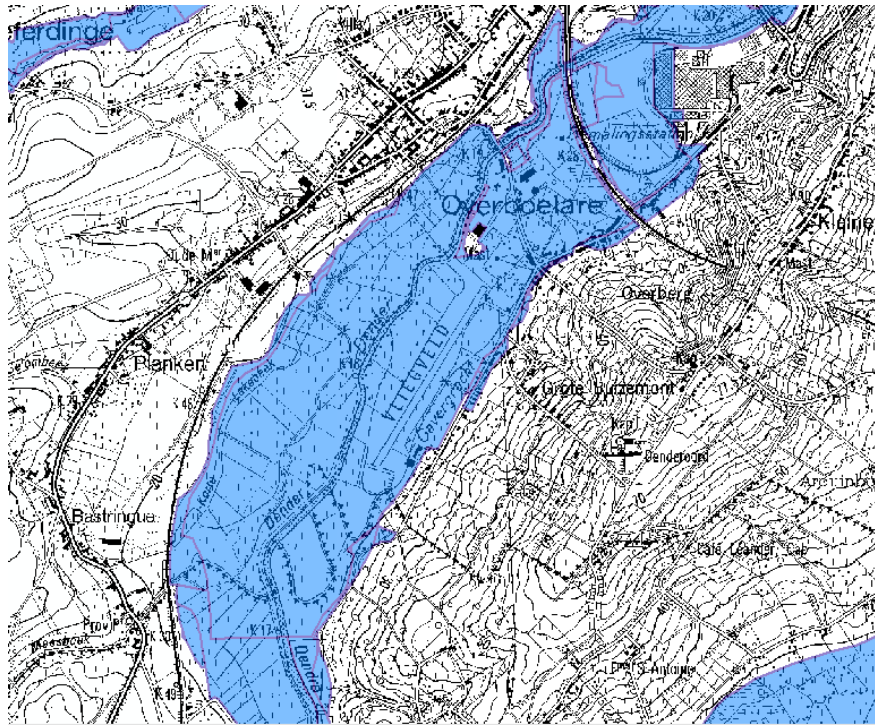


Figure 34 – Inundation areas of the last twenty years (from helicopter images) near Overboelare

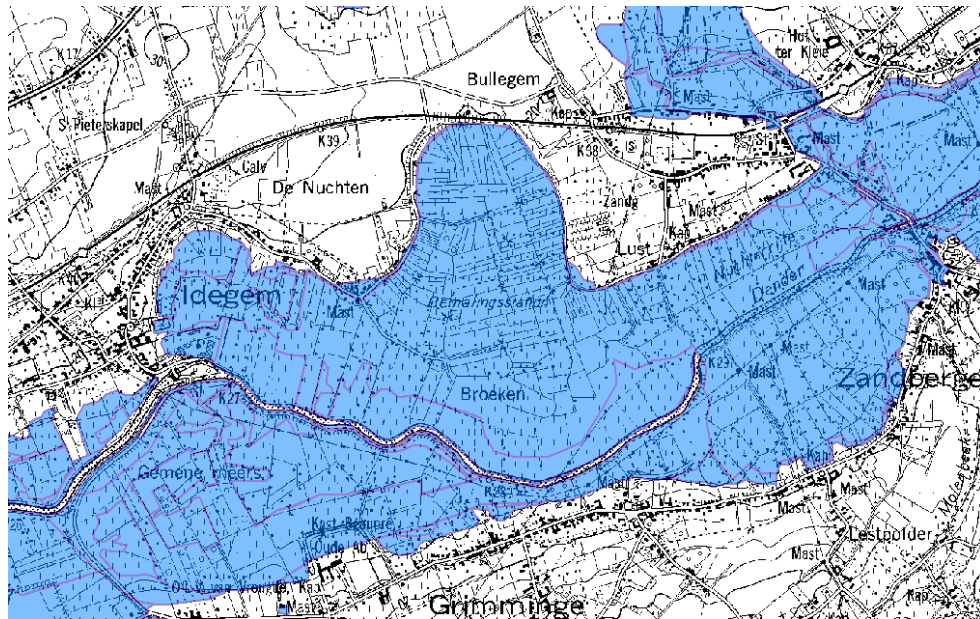


Figure 35 – Inundation areas of the last twenty years (from helicopter images) between Geraardsbergen and Ninove

An additional tool that can help water managers to easily visualize flood zones is the Geographical Information System (GIS) visualization. Indeed, the use of topographic maps containing both natural features and details of urbanized areas can improve the management of the flood risk, especially when (probabilistic) flood maps are produced in real time. Using GIS, different types of information can be assembled and this improves the estimation of the flood extent (see Sanyal & Lu, 2004, for the combined use of remote sensing technology and GIS in flood management). This “integrating technology” (Foote and Lynch, 1995) offered by GIS is nowadays readily possible using software like ArcGIS. In this thesis the central application of ArcGIS, ArcMap, is used to display the necessary layers, i.e. the produced flood maps and the topographic maps corresponding to the study areas.

Figure 36 shows the deterministic flood map obtained with MIKE11, as visualized in ArcMap, after the superimposition of this map with the topographic map of the area near Overboelare. The MIKE11 GIS extension is used for this purpose.

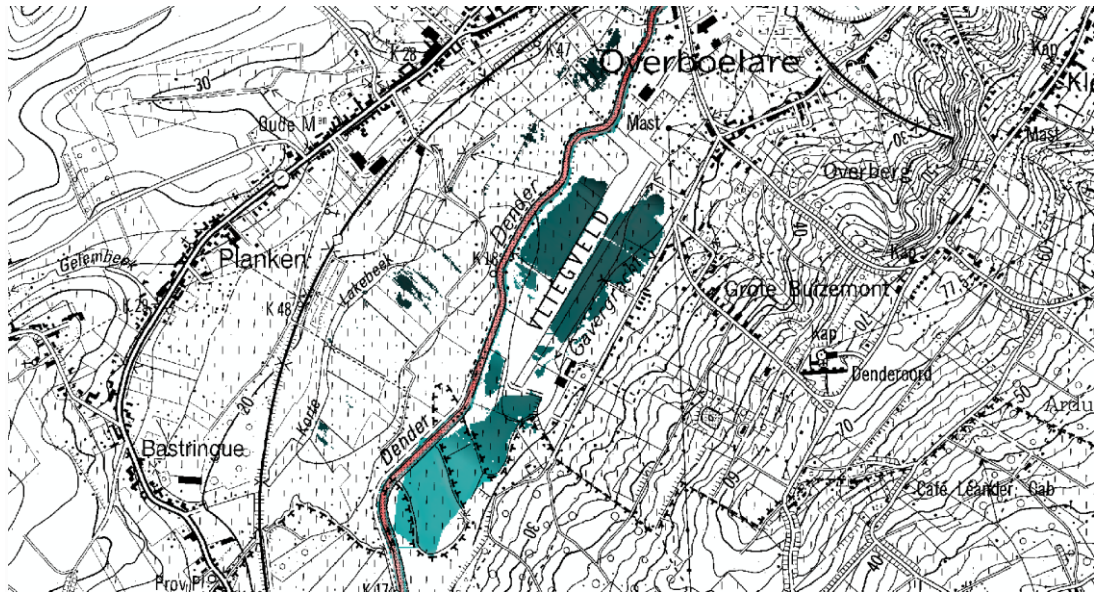


Figure 36 – Deterministic flood map (MIKE11 simulation) superimposed on the topographic map near Overboelare (flood event of June 2016)

Since one of the main aims of this thesis is the production of PFMs, whose advantages (if compared with the deterministic maps) were explained above, the next step consists of displaying the PFMs produced in MATLAB along with the topographic maps of the zones subject to flooding. This is done again using the ArcGIS platform, where the matrix created with MATLAB is imported as a raster containing numbers from 0 to 20 (i.e. the number of intervals considered in the uncertainty propagation phase). Figure 37 and 38 contain the GIS visualization of the two PFMs, previously produced for the flood event of January 2011.

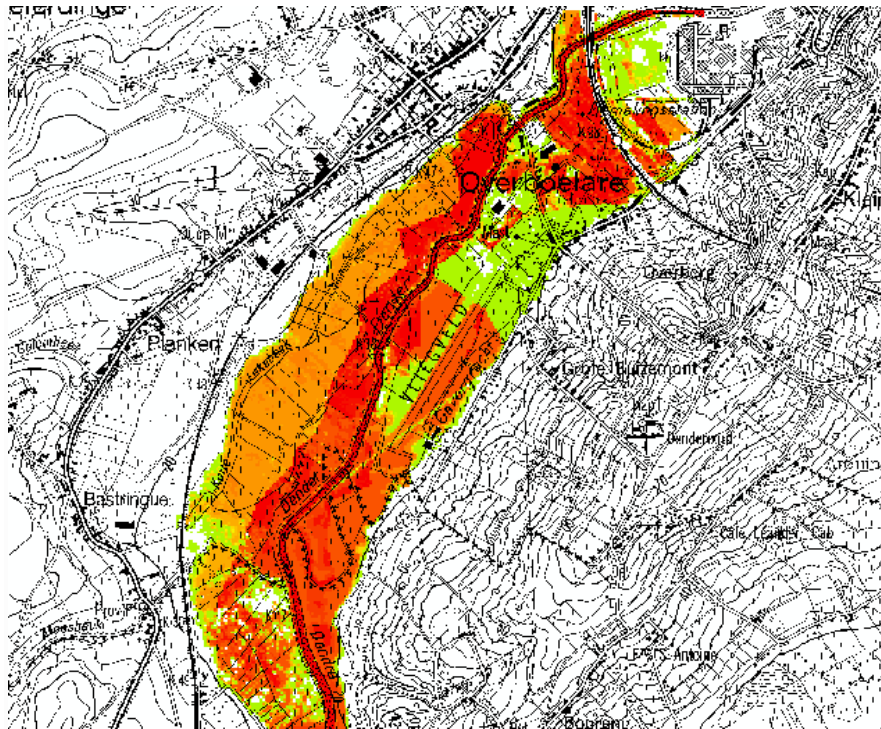


Figure 37 – GIS visualization of PFM, area at the south of Geraardsbergen (flood event of January 2011)

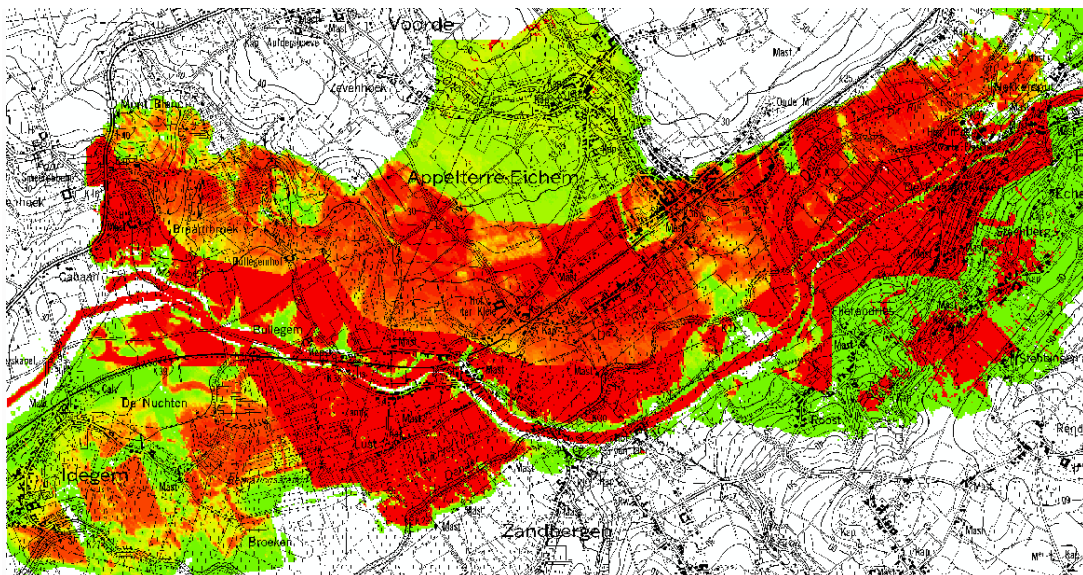


Figure 38 – GIS visualization of PFM, area between Geraardsbergen and Ninove (flood event of January 2011)

The aim of the production of PFMs (including their GIS applications) is to make these maps available online and to update them in real time, so that people could be kept informed about flood risk affecting the area they live in. In this way people could take proactive measures and possibly prepare their property for flooding. At the moment the *waterinfo.be* portal does not provide real time

PFMs in Flanders, but it gives useful information about floods, tides, rainfall and drought. Indeed people can check current situation, short term forecasts (48 hours) or long term forecasts (10 days) in terms of water levels at given gauge stations. The graphs also show the alarm level line for these locations. However, Flemish water managers do not take into account any uncertainty in their forecasts. It is also possible to compare this forecasting system with another European one, like the UK's one. In England, in particular, the Environmental Agency provides 24/7 data that are used to calculate the likelihood of flooding from rivers and the sea. Then different types of information can be found on different websites. For instance, *checkmyfloodrisk.co.uk* shows maps representing different levels of flood risk. Four different classes are identified, according to the chance of flooding: the high risk area, which is defined as the area where the chance of flooding is greater than once every 30 years ($>3.3\%$), the medium risk area ($>1\%$), the low risk area ($>0.1\%$) and finally the very low risk area ($<0.1\%$). Such a service, that also considers flood defences as well as predicted flood levels, definitely increases awareness among the population of the probability of flooding. In addition, *floodalerts.com* website provides real time flood warnings, that are updated every 15 minutes. There is also the possibility for users to monitor a certain location by activating a service that sends them notifications about the developments of flood warnings. Furthermore, people can visit *gaugemap.co.uk*, where they can find detailed information about real time tidal level and river level. Different lines in the graphs indicate whether the river is within the typical range at that gauge station, below this range or whether it is likely to flood.

The shorter the computation time is, the more efficient a system of flood prediction and flood alert like this is. Indeed if simulations are fast, a large number of these can be performed in flood forecasting. This means that it is possible to vary boundary conditions or other parameters and this yields results that take into account different types of uncertainty.

Conclusions

This thesis focuses on the issue of probabilistic river flood modelling and mapping, which is nowadays becoming more and more important due to the expected increase of flood risk, as result of both climate change and socio-economic development.

Different types of modelling were presented. In a first simulation the detailed hydrodynamic model of MIKE11 was used, which turned out to be quite time consuming. Therefore, in order to reduce the computation time, the conceptual modelling approach was considered. The latter showed that the use of the conceptual model doesn't lead to significant loss of accuracy, on the contrary a very good agreement between the results of the two models was obtained. This could be an incentive to use this new technique of modelling in forecasting applications, especially when the results need to be updated in real-time.

Since every model is affected by several sources of uncertainty, the effect of this uncertainty was investigated by propagating it through the model. For the case study in question, the incoming discharge from Wallonia was selected as upstream boundary for which the uncertainty was propagated. The results of the propagation were compared with the real measurements of the gauging station of Overboelare and showed that the measured water levels totally fall in the confidence interval that was produced. On the contrary, the simulated water levels obtained without taking into account any uncertainty, showed underestimated values, especially for peak values, which are definitely the most important ones. Hence, accounting for uncertainty is extremely important in flood modelling. Moreover, the uncertainty propagation was performed making use of the conceptual model, since multiple simulations needed to be run. This highlighted even more the importance of conceptual river models, which make this kind of methodology possible thanks to their very short calculation times. Finally, probabilistic flood maps were produced in order to visualize the uncertainty accounted in the latter step. Again this was done using the results of the uncertainty propagation achieved with the conceptual model. The probabilistic flood maps showed that the extra information about uncertainty can be easily displayed and this can help water managers to mitigate the consequences of dangerous floods.

Appendix

In Table 4 the storage reservoirs that compose the conceptual model of the river Dender are listed, together with the branch name and the chainage of both the most upstream and downstream nodes. In Table 5 the numbers corresponding to the different methods used for the calculation of the water levels and discharges are specified (Meert *et al.*, 2017).

Reservoir number	Branch In	Node In	Branch Out	Node Out	Length	WL Type	Q _{OUT} Type
1	DENDER	0	DENDER	3722	3722	2	3
2	DENDER	3722	DENDER	4900	1178	2	2
3	DENDER	4900	DENDER	5769	869	1	3
4	DENDER	5769	DENDER	8469	2700	2	3
5	DENDER	8469	DENDER	11150	2681	2	2
7	DENDER	11150	DENDER	13950	2800	1	3
8	DENDER	13950	DENDER	17199	3249	2	3
9	DENDER	17199	DENDER	19190	1991	2	2
10	DENDER	19190	DENDER	21660	2470	1	3
11	DENDER	21660	DENDER	24262	2602	2	3
12	DENDER	24262	DENDER	25764	1502	2	3
13	DENDER	25764	DENDER	27220	1456	2	2
14	DENDER	27220	DENDER	29880	2660	2	3
15	DENDER	29880	DENDER	31952	2072	2	3
16	DENDER	31952	DENDER	35990	4038	2	2
17	DENDER	35990	DENDER	38139	2149	1	3
19	DENDER	38139	DENDER	44100	5961	4	2
20	DENDER	44100	DENDER	49500	5400	3	2
21	MARK	20800	MARK	24315	3515	1	1
22	MOLENBEEK_G	0	MOLENBEEK_G	942	942	1	2
23	WOLFPUTBEEK	0	WOLFPUTBEEK	1363	1363	1	3
24	BELLEBEEK	12800	BELLEBEEK	15746	2946	1	2
26	MOLENBEEK2	16400	MOLENBEEK2	23022	6622	1	1
27	FLOODBRANCH4_1	0	FLOODBRANCH4_1	300	300	1	2
28	FLOODBRANCH4_1	300	FLOODBRANCH4_1	1180	880	1	2
29	FLOODBRANCH4_1	1180	FLOODBRANCH4_1	1870	690	1	0
30	FLOODBRANCH4_2	0	FLOODBRANCH4_2	165	165	1	2
31	FLOODBRANCH4_2	165	FLOODBRANCH4_2	373	208	1	2
32	FLOODBRANCH4_2	373	FLOODBRANCH4_2	751	378	1	2
33	FLOODBRANCH4_2	751	FLOODBRANCH4_2	882	131	1	0
34	FLOODBRANCH4_3	0	FLOODBRANCH4_4	50	1844	1	2
35	FLOODBRANCH4_4	50	FLOODBRANCH4_4	400	350	1	2
36	FLOODBRANCH4_4	400	FLOODBRANCH5	384	1030	1	0
37	FB_R_8	0	FB_R_8	1334	1334	1	0
38	FB_R_9	0	FB_R_9	676	676	1	0
39	FB_L_10	0	FB_L_10	5334	5334	1	0
40	FLOODBRANCH3_2	0	FLOODBRANCH3_2	410	410	1	2
41	FLOODBRANCH3_2	410	FLOODBRANCH3_2	2335	1925	1	2
42	FLOODBRANCH3_2	2335	FB_L_6	300	1135	1	2
43	FB_L_6	300	FB_L_6	1399	1099	1	0

44	FLOODBRANCH3_1	0	FLOODBRANCH3_1	2245	2245	1	2
45	FLOODBRANCH3_1	2245	FLOODBRANCH3_1	3725	1480	1	2
46	FLOODBRANCH3_1	3725	FLOODBRANCH2_5	1780	1805	1	2
47	FLOODBRANCH2_1	0	FLOODBRANCH2_1	1806	1806	1	2
48	FLOODBRANCH2_1	1806	FLOODBRANCH2_1	2607	801	1	0
49	FLOODBRANCH2_2	0	FLOODBRANCH2_2	500	500	1	0
50	FLOODBRANCH6_1	0	FLOODBRANCH6_1	2684	2684	1	2
51	FLOODBRANCH6_1	2684	FLOODBRANCH6_1	4704	2020	1	0
52	FLOODBRANCH2_5	1780	FLOODBRANCH2_4	1288	1358	1	2
53	FLOODBRANCH2_4	1288	FLOODBRANCH6_2	1468	1475	1	2
54	FLOODBRANCH6_2	1468	FLOODBRANCH6_2	2530	1062	1	2
55	FLOODBRANCH6_2	2530	FLOODBRANCH6_2	2620	90	1	2
56	FLOODBRANCH6_2	2620	FLOODBRANCH6_2	4305	1685	1	0
57	FB_L_9	0	FB_L_9	1878	1878	1	0
58	FB_R_1	0	FB_R_6	650	1342	1	2
59	FB_R_6	650	FB_R_6	882	232	1	0
60	FLOODBRANCH12_1	0	FLOODBRANCH12_1	548	548	1	0
61	FLOODBRANCH12_2	0	FLOODBRANCH12_2	728	728	1	0
62	FB_L_11	0	FLOODBRANCH11	762	2390	1	2
63	FLOODBRANCH7_2	0	FLOODBRANCH7_2	2553	2553	1	0
64	FB_R_5	0	FB_R_5	845	845	1	2
65	FB_R_5	845	FB_R_5	2859	2014	1	2
66	FB_R_5	2859	FB_R_5	3982	1123	1	0
67	FB_L_12	0	FB_L_12	1225	1225	1	0
68	FB_L_5	0	FB_L_5	599	599	1	0
69	FLOODBRANCH10_2	0	FLOODBRANCH10_2	2100	2100	1	2
70	FLOODBRANCH10_2	2100	FLOODBRANCH10_2	3150	1050	1	2
71	FLOODBRANCH10_2	3150	FLOODBRANCH10_2	3795	645	1	0
72	FLOODBRANCH10_1	0	FLOODBRANCH10_1	1884	1884	1	0
73	FB_R_4	0	FB_R_4	4821	4821	1	0
74	FB_L_4	0	FB_L_4	2262	2262	1	0
75	FB_L_3	0	FB_L_3	596	596	1	0
76	FB_R_3	0	FB_R_3	2200	2200	1	0
77	FB_R_1	0	FB_R_1	2334	2334	1	2
78	FB_R_1	2334	FB_R_1	3671	1337	1	0
79	FLOODBRANCH8	0	FLOODBRANCH8	1824	1824	1	2
80	FLOODBRANCH8	1824	FLOODBRANCH8	4306	2482	1	2
81	FB_L_2	0	FB_L_2	5892	5892	1	0
82	FB_L_1	0	FB_L_1	3748	3748	1	0

Table 4 – Storage reservoirs that compose the conceptual model of the river Dender

WL calc Type		Q calc Type	
1	Hypsometric curve	1	S-Q relation
2	Hypsometric surface	2	Hydraulic Structure
3	Tidal zone	3	Fictitious structure
4	Transition zone		

Table 5 – Methods used to calculate water levels and discharges

Bibliography

Alderman, K., Turner, L. R., Tong, S. L. (2012). Floods and human health: A systematic review. *Environment International*, 47, 37–47

Alfonso, L., M. M. Mukolwe, and G. Di Baldassarre (2016), Probabilistic Flood Maps to support decision-making: Mapping the Value of Information, *Water Resour. Res.*, 52, 1026–1043, doi:10.1002/2015WR017378.

Apel, H., Thielen, A. H., Merz, B., and Blöschl, G. (2004) Flood risk assessment and associated uncertainty, *Nat. Hazards Earth Syst. Sci.*, 4, 295–308.

Arnaud, P., Bouvier, C., Cisneros, L., and Dominguez, R. (2002) Influence of rainfall spatial variability on flood prediction. *Journal of Hydrology*, 260, 216–230, [https://doi.org/10.1016/S0022-1694\(01\)00611-4](https://doi.org/10.1016/S0022-1694(01)00611-4)

Arnell, N., and S. Gosling, The impacts of climate change on river flood risk at the global scale, *Climatic Change* (2016) 134: 387. doi:10.1007/s10584-014-1084-5.

Beven, K., Binley, A. (1992). The future of distributed model: calibration and uncertainty prediction. *Hydrological Processes*, 6, 279-298.

Biggs, E.M., Atkinson, P.M. (2011). A comparison of gauge and radar precipitation data for simulating an extreme hydrological event in the Severn Uplands, UK. *Hydrological Processes*, vol 25, no. 5, pp. 795-810.

Blasone, R.S., Vrugt, J.A., Madsen, H., Rosbjerg, D., Robinson, B.A., Zyvoloski, G.A., (2008). Generalized likelihood uncertainty estimation (GLUE) using adaptive Markov chain Monte Carlo sampling. *Advances in Water Resources*. 31 (4), 630–648.

Bogner, K., Pappenberger, F., Cloke, H. L. (2012). Technical note: The normal quantile transformation and its application in a flood forecasting system. *Hydrology and Earth System Sciences*, 16, 1085-1094.

Box, G.E.P., Cox, D.R., 1964. An analysis of transformations. *Journal of the Royal Statistical Society* 26, 211–243 (Discussion 244–252).

Brandimarte, L., & Di Baldassarre, G. (2012). Uncertainty in design flood profiles derived by hydraulic modeling. *Hydrology Research*, 43(6), 753. doi:10.2166/nh.2011.086.

Demir, V., Kisi, O. (2015). Flood Hazard Mapping by using Geographic Information System and hydraulic model: Mert River, Samsun, Turkey. *Advances in Meteorology*, Volume 2016, Article ID 4891015.

DHI (2011). Mike11: A modelling system for rivers and channels. Reference Manual, DHI Software 2011.

Domeneghetti, A., Vorogushyn, S., Castellarin, A., Merz, B., Brath, A.. (2013). Probabilistic flood hazard mapping: effects of uncertain boundary conditions. *Hydrol. Earth Syst. Sci.*, 17, 3127–314. DOI: 10.5194/hess-17-3127-2013.

Fenton, J. D. (1992). Reservoir routing. *Hydrological Sciences Journal*, 37(3), 233–246. doi:10.1080/02626669209492584.

Foote, Kenneth E., Lynch, M.. (1995) *The Geographer's Craft Project*, Department of Geography, The University of Colorado at Boulder.

Gabriele S., Chiaravalloti, F., Procopio, A. (2017). Radar–rain-gauge rainfall estimation for hydrological applications in small catchments. *Avances in Geosciences*, 44, 61-66.

Gharbi, M., Soualmia, A., Dartus, D., Masbernat, L. (2016). Comparison of 1D and 2D Hydraulic Models for Floods Simulation on the Medjerda River in Tunisia. *J. Mater. Environ. Sci.* 7 (8) 3017-3026.

Golasowski, M., Litschmannova, M., Kuchar, S., Podhoranyi, M. & Martinovic, J. (2015). Uncertainty modelling in rainfall-runoff simulations based on parallel Monte Carlo method. *International Journal on non-standard computing and artificial intelligence NNW* .

Hall, J., Solomatine D., (2008). A framework for uncertainty analysis in flood risk management decisions. *International Journal of River Basin Management*, 6:2, 85-98.

Huang Y, Chen X, Li YP, Huang GH, Liu T (2010) A fuzzy-based simulation method for modelling hydrological processes under uncertainty. *Hydrol Process* 24: 3718–3732. DOI: 10.1002/hyp.7790.

Jarrett, R. D. (1985). Determination of roughness coefficients for streams in Colorado. *Water-Resources Investigations Report 85-4004*.

Jung, Y. (2011). Uncertainty in Flood Inundation Mapping. Ph.D. Thesis, Purdue University Graduate School, Purdue, IN, USA.

Li, Y., Grimaldi S., Walker J., Pauwels V. (2016). Application of remote sensing data to constrain operational rainfall-driven flood forecasting: a review. *Remote Sensing*, 8:456.

Maskey, S., Guinot, V. and Price, R.K. (2004). Treatment of Precipitation Uncertainty in Rainfall-Runoff Modelling: A Fuzzy Set Approach. *Advances in Water Resources*, 27, 889–898.

Meert, P.; Willems, P.; Nossent, J.; Vanderkimpen, P.; Pereira, F.; Verwaest, T.; Mostaert, F. (2016). Development of conceptual models for an integrated catchment management: Subreport 3 – Construction and calibration of conceptual river models. Version 4.0. WL Rapporten, 00_131. Flanders Hydraulics Research: Antwerp, Belgium.

Meert, P., Pereira, F., Willems, P. (2016-b). Uncertainty assessment of river water levels on energy head loss through hydraulic control structures. Erpicum, S. et al. (Ed.) *Proceedings of the 4th IAHR Europe Congress, Liege, Belgium, 27-29 July 2016: Sustainable Hydraulics in the Era of Global Change*. pp. 863-870

Meert, P.; Willems, P.; Nossent, J.; Vanderkimpen, P.; Pereira, F.; Verwaest, T.; Mostaert, F. (2017). Development of conceptual models for an integrated catchment management: Subreport 4 – Uncertainty analysis. Version 1.0. WL Rapporten, 00_131. Flanders Hydraulics Research: Antwerp, Belgium.

Montanari A. (2007). What do we mean by ‘uncertainty’? The need for a consistent wording about uncertainty assessment in hydrology. *Hydrological Processes*, 21, 841-845.

Muis, S., Güneralp, B., Jongman, B., Aerts, J. C. J. H., & Ward, P. J. (2015). Flood risk and adaptation strategies under climate change and urban expansion: A probabilistic analysis using global data. *Science of the Total Environment*, 538, 445-457. DOI: 10.1016/j.scitotenv.2015.08.068.

Nash, J. E., & Sutcliffe, J. V. (1970). River flow forecasting through conceptual models. Part 1 - A discussion of principles. *Journal of Hydrology*, (10), 282–290.

Pappenberger, F., Beven, K., Horritt, M., Blazkova, S. (2005). Uncertainty in the calibration of effective roughness parameters in HEC-RAS using inundation and downstream level observations, *J. Hydrol.*, 302, 46–69, doi:10.1016/j.jhydrol.2004.06.036.

Bell, R., Lawrence, J., Allan, S., Blackett P., Stephens S. (2017). Coastal hazards and climate change. Guidance for local government. New Zealand: Ministry for the Environment.

Sanyal, J., Lu X.X. (2004). Application of remote sensing in flood management with special reference to Monsoon Asia: A review. *Natural Hazards*, 33: 283.

Shrestha, D.L, Rodriguez, J., Price, R.K. and Solomatine, D.P. (2006). “Assessing Model Prediction Limits Using Fuzzy Clustering and Machine Learning,” *Proceedings of the Int. Conf. on Hydroinformatics*, Nice, France

Shrestha, D. L.; Solomatine D. P. (2008) Data-driven approaches for estimating uncertainty in rainfall-runoff modelling, *International Journal of River Basin Management*, 6:2, 109-122, DOI: 10.1080/15715124.2008.9635341.

Van Den Zegel, B., Vermuyten, E., Wolfs, V., Meert, P., Willems, P. (2014). Real-time control of floods along the Demer River, Belgium, by means of MPC in combination with GA and a fast conceptual river model. *Proceedings of 11th International Conference on Hydroinformatics (HIC 2014)*. New York, USA.

Van der Waerden, B.L., 1952. Order tests for two-sample problem and their power I. *Indagationes Mathematicae* 14, 453e458.

Van Steenbergen, N., Ronsyn, J., & Willems, P. (2012). A non-parametric data-based approach for probabilistic flood forecasting in support of uncertainty communication. *Environmental Modelling and Software* , 33, 92–105. doi:10.1016/j.envsoft.2012.01.013

Van Steenbergen, N. (2014). Uncertainty quantification and reduction for river flood forecasting. PhD-dissertation. KU Leuven.

Van Steenberghe, N., Willems, P. (2014). Uncertainty decomposition and reduction in river flood forecasting: Belgian case study. *Journal of Flood Risk Management*.

Vermuyten E., Van den Zegel B., Wolfs V., Meert P. and Willems P. (2014). Real-time flood control by means of an improved MPC-GA algorithm and a fast conceptual river model for the Demer basin in Belgium. 6th International Conference on Flood Management, Sao Paulo, Brazil, 16-18 September 2014.

Willems, P. (2000). Probabilistic immission modelling of receiving surface waters. PhD-dissertation. KU Leuven.

Willems P., G. Vaes, D. Popa, L. Timbe & J. Berlamont (2002). Quasi 2D river flood modelling. River Flow 2002. D. Bousmar and Y. Zech (ed.), Swets & Zeitlinger, Lisse, Volume 2, 1253-1259.

Willems, P. (2009). A time series tool to support the multi-criteria performance evaluation of rainfall-runoff models. *Environmental Modelling & Software*, 24(3), 311–321.

Wolfs, V., Meert, P., & Willems, P. (2015). Modular conceptual modelling approach and software for river hydraulic simulations. *Environmental Modelling & Software*, 71, 60–77. doi:10.1016/j.envsoft.2015.05.010

Yankovsky, A. E., Torres, R., Torres-Garcia, L. M., Jeon, K., 2012. Interaction of tidal and fluvial processes in the transition zone of the Santee River, SC, USA. *Estuaries and Coasts*, 35 (6), 1500-1509.

Sitography

Baumann, J., 2016. Flood forecast maps safeguard Belgium. Available at: <http://www.esri.com>. Accessed 1 February 2018

CH2M, 2017. Available at: <https://www.floodmodeller.com/help-support/videos/videos-webinars/> Accessed 7 February 2018.

DHI, 2017. Hydrodynamics: advanced 2D and 3D modelling of hydrodynamic processes. Available at:

<https://www.mikepoweredbydhi.com/products/mike-21/hydrodynamics>.
Accessed 15 February 2018

European Commission, Flood mapping: a core component of flood risk management. Available at:
http://ec.europa.eu/environment/water/flood_risk/flood_atlas/
Accessed 10 January 2018

Flemish Environment Agency, 2012. Twenty years of flood experience in Flanders (Belgium). Available at:
https://keynote.conference-services.net/resources/444/2653/pdf/IWAWCE2012_0781.pdf
Accessed 1 February 2018